Chem Soc Rev

REVIEW ARTICLE

View Article Online
View Journal | View Issue

Cite this: *Chem. Soc. Rev.*, 2024, 53, 8847

Biomaterials with cancer cell-specific cytotoxicity: challenges and perspectives

Zhaoyou Chu,†[ab] Wanni Wang,†[a] Wang Zheng,†[a] Wanyue Fu,†[a] Yujie Wang,†[a] Hua Wang*[b] and Haisheng Qian *[ac]

Received 21st June 2024

DOI: 10.1039/d4cs00636d

rsc.li/chem-soc-rev

Significant advances have been made in materials for biomedical applications, including tissue engineering, bioimaging, cancer treatment, *etc.* In the past few decades, nanostructure-mediated therapeutic strategies have been developed to improve drug delivery, targeted therapy, and diagnosis, maximizing therapeutic effectiveness while reducing systemic toxicity and side effects by exploiting the complicated interactions between the materials and the cell and tissue microenvironments. This review briefly introduces the differences between the cells and tissues of tumour or normal cells. We summarize recent advances in tumour microenvironment-mediated therapeutic strategies using nanostructured materials. We then comprehensively discuss strategies for fabricating nanostructures with cancer cell-specific cytotoxicity by precisely controlling their composition, particle size, shape, structure, surface functionalization, and external energy stimulation. Finally, we present perspectives on the challenges and future opportunities of nanotechnology-based toxicity strategies in tumour therapy.

1. Introduction

Although current clinical oncology treatments have made significant progress, shortcomings and challenges still exist, including potential systemic toxicity, low bioavailability, potential complications, and possible disease recurrence.[1–3] Materials medicine has been developed in the past few decades to improve cancer treatment efficacy and provide new forms of precision medicine and personalised treatment.[4–7] Nanocarriers offer many advantages in oncology therapy, including targeted drug delivery, increased drug solubility, prolonged circulation time, drug payload protection, and multiple pharmacological functionalities.[8–14] However, they possess limitations, including complex formulations, biocompatibility and toxicity issues, inadequate biodistribution, and limited drug loading capacity. More than 20

[a] *School of Biomedical Engineering, Anhui Provincial Institute of Translational Medicine, Anhui Medical University, Hefei, Anhui 230032, P. R. China. E-mail: shqian@ahmu.edu.cn*

[b] *The First Affiliated Hospital of Anhui Medical University, Hefei 230022, P. R. China. E-mail: wanghua@ahmu.edu.cn*

[c] *Anhui Engineering Research Center for Medical Micro-Nano Devices, Anhui Medical University, Hefei 230011, P. R. China*

† These authors contributed equally to this work.

Zhaoyou Chu

Dr Zhaoyou Chu obtained his BS degree from Anhui University (2016) and PhD degree (2023) from Anhui Medical University under the supervision of Prof. Haisheng Qian. Currently, he works at the First Affiliated Hospital of Anhui Medical University as a postdoctoral fellow. His research focuses on the development of various multi-functional nanomaterials for treatment of cancer, wound infection and wound repair.

Wanni Wang

Dr Wanni Wang obtained her BS degree from Anhui University (2015) and PhD degree (2021) from Hefei University of Technology under the supervision of Prof. Haisheng Qian. Currently, she is an Associate Professor at the School of Biomedical Engineering, Anhui Medical University. Her research focuses on the development of bioactive materials for biomedical applications, including cancer therapy, sterilization and bioimaging.

nanomedicines have been approved for cancer therapy worldwide (Table 1).

Materials used in cancer treatment require good biocompatibility with normal cells or tissues and excellent killing ability against cancer cells. Materials with specific toxicity to cancer cells can be tailored by adjusting their structure, size, particle size, and surface characteristics.[15,16] For example, iron oxide nanoparticles (NPs), which have good biocompatibility, magnetic properties, and surface modification capacity, can utilise the characteristic acidity of a tumour microenvironment and its excess hydrogen peroxide (H_2O_2) to catalyse the Fenton reaction and achieve specific therapeutic effects.[17]

Nanostructured materials display chemical activities or interactions with cancer cells or tissues that are tunable by adjusting their size, shape, and structures. Excitation under external physical stimuli such as light, sound, magnetic and electrical fields, and force may also lead to local and precise treatments.[18–22] In addition, heterogeneity among different tumours and within the same tumour may also affect biomaterial delivery and targeting effectiveness, as different cells may have different biomaterial uptakes and responses. More importantly, although some biomaterials have strong clinical translational potential, their biological effects, especially their long-term effects and tolerability, need further evaluation before clinical translation.

In this review, we firstly discuss the responsiveness principles of materials medicine at the cellular and tissue levels. We then highlight recent advances in the design of these biomaterials, including their composition, particle size, shape, structure, and surface functionalization. Some challenging obstacles have been overcome. We aim to uncover the potential of biomaterials to transform the therapeutic landscape and

Wang Zheng

Mr Wang Zheng received his BS degree in Biomedical Engineering from Anhui Medical University in 2022. In the same year, he pursued his master's degree and joined the Biomedical Materials Research and Engineering Transformation Laboratory of Anhui Medical University under supervision of Prof. Haisheng Qian. Currently, his research interest mainly focuses on the synthesis of inorganic nanomaterials and the biological applications of tumor diseases.

Wanyue Fu

Ms Wanyue Fu graduated in Biomedical Engineering from Wannan Medical College in 2022. In September of the same year, she joined the Biomedical Materials Research and Engineering Transformation Laboratory of Anhui Medical University directed by Prof. Haisheng Qian. Her current research interest focuses on the synthesis of nanomaterials and the application of nanomaterials in inflammatory bowel disease.

Yujie Wang

Mr Yujie Wang obtained his BS degree from Chizhou University (2020). In 2022, he joined the Prof. Haisheng Qian's group pursuing his master's degree at Anhui Medical University. Currently, his research interest is focused on the design of various biomaterials for biomedical applications, including cancer treatment, anti-inflammatory, and diabetic rupture.

Hua Wang

Dr Hua Wang is currently a professor at the Institute for Liver Disease at Anhui Medical University. He is also Chief, Division of Tumor Immunotherapy in the Department of Oncology, and also the Director of biobank of the First Affiliated Hospital of Anhui Medical University. He received his MD and PhD from Anhui Medical University followed by clinical and research training. Dr Wang pursued his post-doctoral trainings in Dr Bin Gao's lab at NIAAA/NIH for almost 7 years. His main interest is liver injury and repair. He is the author of more than 100 peer-reviewed publications in the highly prestigious journals including Gastroenterology, Hepatology, Journal of Hepatology and PNAS. In the past several years, he received several grant support from national and provincial natural science foundation of China.

Table 1 List of approved nanomedicines for cancer treatment

Medicines	Drug carriers	Indications	Approval date	Corporation
Smancs	Commercial molecules make new oncostatin couplers	Liver and kidney cancer	1993	Astellas Pharma Inc
Oncaspar	Commercial protein coupling	Acute lymphoblastic leukemia	1994	Sigma Tau
Doxil (Caelyx)	Polyethylene glycolised doxorubicin liposome	Ovarian cancer and breast cancer	1995	Yang Sen
DaunoXome	Liposomes of soft red plum	HIV-associated Kaposi's sarcoma	1996	GALEN
DepoCyt	Alfucoside liposome	Lymphoma meningitis	1999	Pacira Pharms
Ontak	Interleukin 2 and diphtheria toxin fusion protein	Cutaneous T-cell lymphoma	1999	Eisai
Rapamune	Sirolimus oral solution	Lymphangioleiomyomatosi0073	1999	Pfizer
Myocet	Doxorubicin liposome	Lymphoma	2000	Teva Pharmaceutical Industries Limited
Eligard	Leuprolide acetate polymer	Prostate cancer	2002	Tolmar Therap
Lipozide	Paclitaxel liposome	Breast, lung, and ovarian cancers	2003	Nanjing Luye Pharmaceutical
Abraxane	Albumin-bound paclitaxel nanospheres	Multiple cancers and metastatic pancreatic cancer	2005	Abraxis Bioscience
Genexol PM	Paclitaxel micelle formulation	Breast cancer and small cell lung cancer	2007	Samyang
Nanoxe	Non-albumin-bound paclitaxel nanoparticles	Breast cancer, pancreatic cancer, and NSCLC	2008	Nanotherapeutics
Mepact	Cytosolic acetyl tripeptide phosphatidylethanolamine liposomes	Osteosarcoma	2009	Takeda
NanoTherm	Iron oxide nanoparticles	Glioblastoma	2010	MagForce
Marqibo	Vincristine liposome	Leukaemia	2012	ACROTECH
DocetaxelPM	Polyene paclitaxel	Breast cancer, gastric cancer, NSCLC, ovarian cancer, prostate cancer, and squamous cell cancer	2013	Lupin Limited
Onivyde	Irinotecan liposome	Pancreatic knee cancer	2015	IPSEN
Vyxeos	Cytarabine and liposomes of *Mycobacterium flexneri*	Acute myelogenous leukemia	2017	Celator Pharms
Apealea	Taxol micelles	Ovarian cancer	2018	PAION AG
Hensify	Hafnium oxide nanopreparations	Locally advanced soft tissue sarcoma	2019	AstraZeneca
Fyarro	Sirolimus protein-bound particles	Malignant perivascular epithelioid cell tumour	2021	Jazz Pharmaceuticals

contribute to the realisation of more efficacious and patient-centric cancer treatments (Fig. 1).

Haisheng Qian

Prof. Haisheng Qian received his BS in chemistry from Anhui University (2000), and PhD degree from the University of Science and Technology of China under the supervision of Prof. Shu-Hong Yu in 2006. And then, he moved to Nanyang Technological University (2006–2007) and National University of Singapore (2007–2009) and worked as a postdoctoral fellow. Currently, he is a Full Professor and Dean of the School of Biomedical Engineering, Anhui Medical University. In 2022, he was selected as the Fellow of the Royal Society of Chemistry (FRSC). He has authored and co-authored more than 220 peer reviewed international journal papers. His research interests include the synthesis and delivery of multi-functional bioactive materials for antibacterial applications, cancer therapy and bioimaging.

2. Biomaterial responsiveness principles *in vitro* and *in vivo*

Material medicines provide new methods for precision medicine and personalised treatment that require a deeper understanding of the interaction mechanisms. In this section, we illustrate the differences at the tumour cellular level (such as glucose, lactate, reactive oxygen species (ROS), glutathione (GSH), and folate) and tissue level (such as the extracellular matrix (ECM), vascular system, immune cells, stromal cells, acidic environment, and production of hydrogen sulphide (H_2S)) compared to normal cells and tissues and describe how they are leveraged to design nanostructured materials with high specific cytotoxicity (Fig. 2).

2.1. Cellular level

At the cellular level, tumour cells lose the strict growth and division regulation of normal cells and divide without restriction, leading to growth, maturation, metastasis, and tumour enlargement. Therefore, tumour cells differ from normal cells in that they display metabolic changes and dependencies to meet the biological energy requirements of rapid growth. They use glucose as the energy source to drive their rapid proliferation and support rapid cell division by producing more lactate.[23] Because their adenosine triphosphate (ATP)

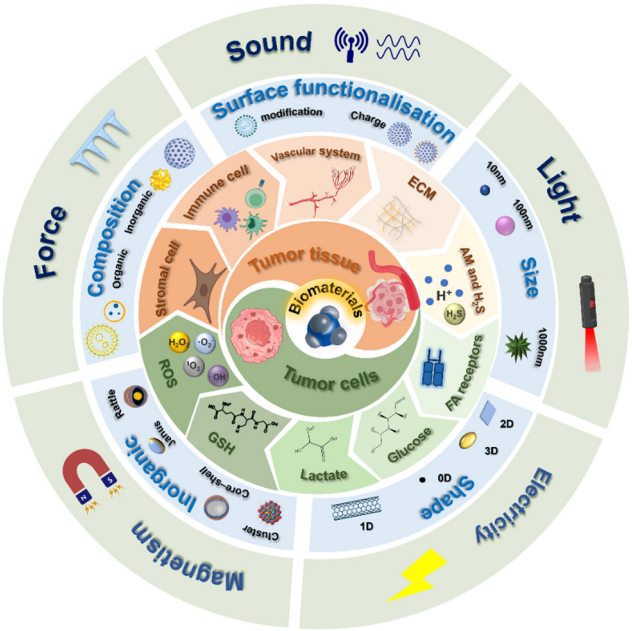

Fig. 1 Schematic illustration of cancer therapy applications based on specific toxicity in terms of tumour and normal cell-to-tissue differentiation and the construction of nanostructured materials.

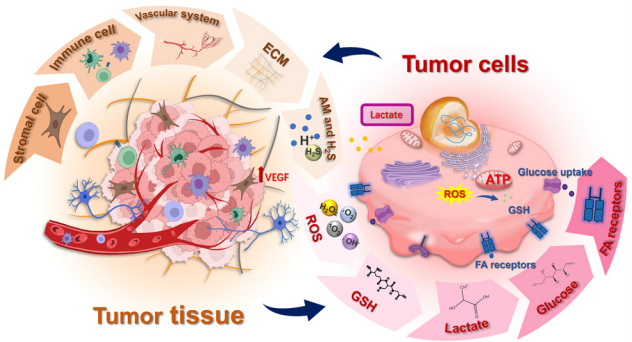

Fig. 2 Summary of responsive therapeutic strategies based on cellular- and tissue-level differential characteristics.

production from glycolysis is low, tumour cells must take up more glucose through compensatory mechanisms (the Warburg effect), making them more susceptible to glucose limitation. As a result, glucose deprivation-based cancer starvation therapies are emerging as effective approaches for inhibiting tumour growth and survival.

Elevated extracellular lactate levels induce the secretion of vascular endothelial growth factors, leading to increased angiogenesis, tumour invasion, and metastasis. Moreover, lactate provides metabolic support for tumour-infiltrating regulatory T cells and interferes with immune responses against cancer. Therefore, lactate is also considered an effective target for regulating aberrant tumour microenvironment (TME) metabolism by blocking lactate production or direct consumption. The elevated lactate levels and other factors, such as an irregular vascular morphology and a hypoxic state, produce an acidic microenvironment, which has multiple effects on tumour cell survival, invasiveness, and drug resistance. Moreover, during tumour maturation, some signaling molecules, such as ROS, are produced in large quantities to activate cell signaling pathways, such as cell proliferation, differentiation, and apoptosis.[24] (We conducted a corresponding review earlier of strategies to modulate H_2O_2 in tumour therapy.[25]) Meanwhile, to control the oxidative damage effects of ROS, the antioxidant system also produces system antioxidants (catalase (CAT), GSH, and thioredoxin reductases (TrxR)) to balance the TME redox homeostasis.[26] For example, GSH is an important antioxidant that reacts to neutralise ROS, thereby reducing intracellular oxidative damage. GSH levels increase in tumour cells to adapt to oxidative stress.

At a certain level of tumour growth, due to the lack of adhesion molecules (such as integrins, selectins, cadherins, and members of the immunoglobulin superfamily (IgSF) including nectins and mucins) that lead to stickiness, the cells can invade surrounding tissues and organs and even spread to distant sites through the blood or lymphatic system to form metastases.[27–31] This ability to invade and metastasise not only makes tumours more dangerous, but also makes certain receptors or antigens (targets) on the surface of tumour cells particularly important.[32] As shown in Fig. 3 and Table 2, compared with normal cells, tumour cells often have high expression of some receptors or antigens (targets), such as the folate receptor (FAR), transferrin receptor (TFR), lectin receptor, epidermal growth factor receptor (EGFR), vascular endothelial growth factor receptor (VEGFR), platelet-derived growth factor receptor (PDGFR), Toll-like receptor (TLR), cell adhesion molecule (CAM) receptor, and prostate-specific membrane antigen (PSMA).[33] Therefore, targeting tumour cell surface receptors can distinguish between tumour and normal cells for specific delivery of killing agents.[34–36]

2.2. Tissue level

At the tissue level, the ECM, tumour vasculature, stromal cells (SCs), and immune cells of the TME exhibit significant variability. SCs include fibroblasts, mesenchymal stromal cells, pericytes, and adipocytes; immune cells include T and B

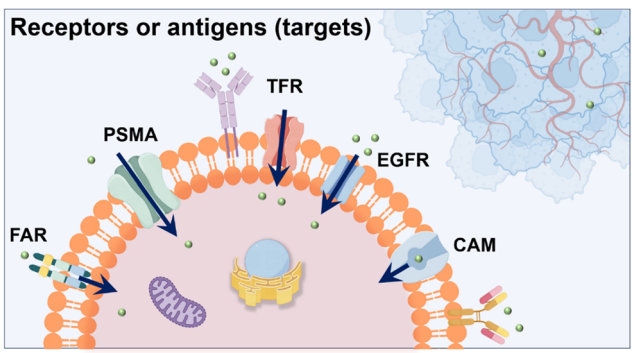

Fig. 3 Schematic representation of tumour cell surface receptors.

Table 2 List of targeting ligands, specific targets, and the targeted cancer types[33]

Ligand type	Target	Location	Cancer types
Small molecules			
Folate acid (FA)	FAR	Cell membrane	Ovarian, uterus, testicular, lung, brain, and pituitary cancers
ACUPA	PSMA	Cell membrane	Prostate cancer
Sulfonamides	CA-IX	Cell membrane	Hypoxic tumours
Benzamides	Sigma receptor	Cell membrane	Melanoma, NSCLC, breast cancers of neural origin, and prostate cancers
Peptides			
iRGD	αvβ3/5	Cell membrane and tumour vascular	Melanoma, glioma, pancreatic, prostate, ovarian, cervical, and breast cancers
LyP-1	gC1qR (p32)	Tumour lymphatics	Lymphatic metastatic tumours
NGR peptide	Aminopeptidase N	Tumour vascular and tumour cell membranes	Vascular in solid tumours
Aptides	Fibronectin	Tumour-associated ECM	Glioma
Proteins			
Transferrin	Transferrin receptor	Cell membrane and tumour vascular	Ovarian, lung, colon, and brain cancers
Albumin	gp60	Caveoli and cell membranes	Vascular targeting in malignant liver cancer and brain cancer
Insulin	IGF-1R	Cell membrane	Lungs, pancreas, and breast cancer
Affibodies	HER2	Cell membrane	$HER2^{+}$ breast cancer
Ankyrin repeat protein	EpCAM Epithelial	Cell membrane	Colon, stomach, prostate, breast, and lung cancers
Antibodies and fragments			
Full antibody	PSMA, EGFR, VEGFR	Cell membrane	Prostate cancer
F(ab′), F(ab′)2, or scFv	HER2, GAH, PD1	Cell membrane	Breast cancer and gastric cancer
Aptamers and antisense oligonucleotides			
A10 (CGA)	PSMA	Cell membrane	Prostate cancer
Ab aptamers	MUC1	Cell membrane	Breast and bladder cancers
Erbitux aptamers	EGFR	Cell membrane	Metastatic colorectal cancer
Carbohydrates			
Mannose	Lectins	Macrophages and liver endothelial cells	—
Glucose (analogs)	GLUT1	Brain capillaries	Glioma
Galactose	Galectin-1 receptor	Hepatocytes	Hepatoma carcinoma

lymphocytes, tumour-associated macrophages (TAMs), myeloid-derived suppressor cells (MDSCs), neutrophils, dendritic cells (DCs), T-lymphocytes, and natural killer (NK) cells.

Produced by multiple cell types in the TME, the ECM not only provides structural support but also provides tumour cells with signals to maintain proliferation, evade growth inhibitory factors, resist cell death, achieve replicative immortality, induce angiogenesis, promote invasion and metastasis, and play an important role in tumour progression.[37–39] Therefore, attacking the ECM in the area of tumour cells is a possible tumour treatment. Current strategies include degrading different ECM components, direct inhibition of the *ab initio* ECM component synthesis, and modifying enzymes essential for secretion and maturation. However, the ECM is tailored to the specific organ function, and local regulation renders the ECM more complex and difficult to target as the tumour progresses. Consequently, far from avoiding tumour progression, treatment may induce metastasis.[40,41]

Compared with healthy tissues, tumour vascular systems are often distorted and dysfunctional, exhibiting uneven vascular permeability.[42] This abnormal vascular system is associated with increased cancer aggressiveness. In addition, dysfunctional blood vessels may selectively block infiltration of specific immune cell types, including cytotoxic T lymphocytes, and significantly interfere with therapeutic drug delivery and distribution.[43,44] Most efforts in this area have targeted the vascular system from two different perspectives: vascular depletion using antiangiogenic therapies and improving drug delivery through vascular normalisation.[45–48]

Metabolic shifts under hypoxia in TME are regulated primarily by the transcription factor hypoxia-inducible factor-1 (HIF-1).[49–52] Because tumour hypoxia can promote its growth and render its cells more treatment-resistant, some drugs have been developed to treat HIF-1 dysregulation in the clinic. However, their therapeutic effect is often minimal because of ineffective drug delivery or drug resistance development after prolonged use. To this end, researchers have attempted to improve drug delivery and chemotherapy (CDT) resistance to achieve differential killing of tumour cells.

The irregular vascular structure within tumour tissue, in conjunction with highly permeable capillaries and the lack of a lymphatic system, contributes to the tumour-enhanced permeability and retention (EPR) effect, which in some cases results in easier entry and retention of drugs and NPs inside the tumour tissue.[53–55] However, preclinical and clinical studies have shown that nanomedicine delivery efficiency to tumours is still unsatisfactory. Some data suggest that nanocarriers only deliver approximately 0.7% of the drug to the tumour tissue.[56–58] This finding raises the question of whether other unrecognised mechanisms impede nanomedicine extravascular penetration at the nonendothelial cell barrier level. The existence of transient, potent pathways through vascular bursts in the tumour vasculature has recently attracted interest, expanding the possibilities for controlled nanomedicine

distribution. Igarashi *et al.* found that dextran, polymeric micelles, liposomes, and polymeric vesicles with diameters ranging from 32 to 302 nm were co-localised in almost all vascular bursts.[59] By mathematical modeling, burst sizes were estimated to be 625 nm or larger, suggesting the dynamic, stochastic formation of large infiltration pathways in the tumour vasculature system. Some bursts were micrometer-sized, allowing the delivery of 1-micron microspheres. Antibody drugs and platelets can be transported *via* vascular bursts, demonstrating the application of this phenomenon to other types of therapeutic and cellular components. These findings demonstrate the great potential of vascular bursting and extend the biological and therapeutic significance of this phenomenon to a wide range of blood-derived particles and cells. Miller *et al.* and Liu *et al.* exploited the effect of post-irradiation TAM accumulation primarily in the microvascular system vicinity, causing dynamic extravasation bursts to enhance drug uptake by neighbouring tumour cells.[60,61] Using a proprietary multilevel *in vivo* imaging technique, Wang *et al.* showed for the first time that a dense basement membrane structure exists on the outside of tumour blood vessels, which severely impedes the extravascular penetration of nanomedicines, leading to the formation of ''blood pools'' of nanomedicines outside the tumour blood vessels.[62] Degradation of the basement membrane by collagenase significantly reduced blood pool formation and effectively enhanced nanoparticle tumour penetration. Finally, they found that acute inflammation induction could enhance the tumour vasopurge effect of nanomedicines. Setyawati *et al.* investigated another form of endothelial leakiness, independent of cellular toxicity and oxidative stress, and dubbed this phenomenon the NanoEL effect.[63] This is also a direct effect of NPs on endothelial cells rather than a secondary effect such as oxidative stress or cell death. This form of endothelial leakage relies on the disruption of vascular endothelial cadherin (VE-cadherin), coupled with actin remodelling and cell shrinkage, inducing micrometer-scale gaps between endothelial cells.

Up to date, many studies have shown that inorganic NPs can contribute to vascular leakage through different mechanisms. Most of these studies have attributed endothelial leakage to mechanisms such as cytoskeletal remodelling and VE-cadherin disruption. Therefore, as shown in Fig. 4, EPR, dynamic burst (DB), and NanoEL are introduced and summarised in more detail.

A connection exists between the EPR effect and protein crowns, particularly in nanoparticle drug delivery. Protein crowns are protein molecules adsorbed or bound to NP surfaces and can be derived from plasma, extracellular fluid, and so on. Protein crowns can influence nanoparticle interactions and behaviour in the context of the EPR effect, which can further affect nanoparticle penetration and retention in tumour tissues. In addition, protein crowns can influence NP interactions with tumour cells or tumour mesenchyme, further affecting their retention time and penetration depth in tumour tissue.[64] Chen *et al.* have long worked to establish analytical methods for nanoprotein crowns and their chemical/biological effects, including the chemical/biological characterisation of nanoprotein crowns, their distribution *in vivo*, and the detection of their transformation products.[65–67] However, protein crowns may facilitate NP penetration and sometimes reduce their targeting properties, as protein adsorption may obscure the targeting ligands on the particle surface. Therefore, the effects of protein crowns must be comprehensively considered when designing nanoparticle drug delivery systems to optimise therapeutic efficacy and targeting.

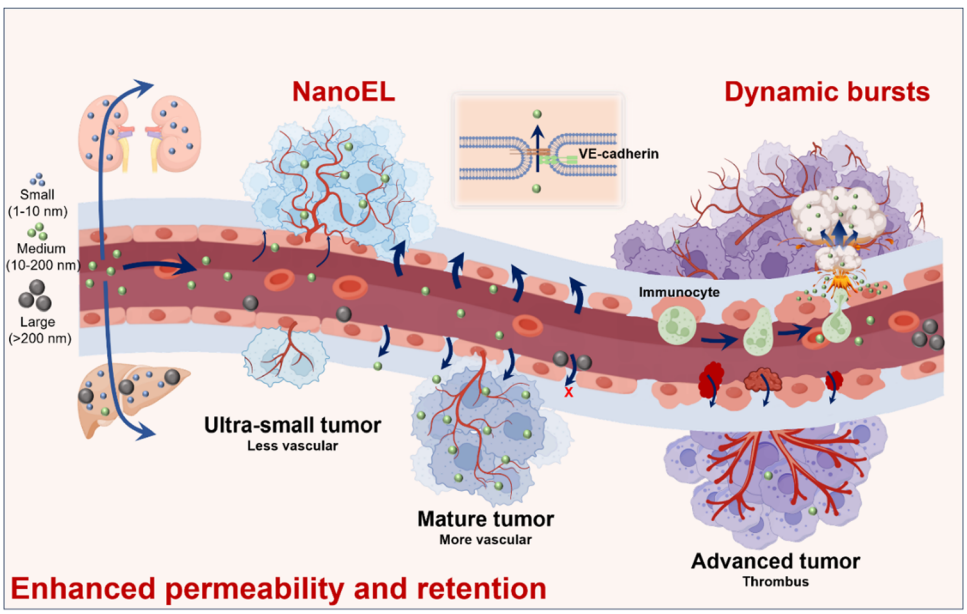

Fig. 4 Schematic representation of the enhanced permeability and retention (EPR), dynamic burst (DB), and NanoEL effects.

Cancer-associated fibroblasts (CAFs) account for more than 50% of SCs. They inhibit immune cell functions by secreting cytokines or metabolites and promote tumour development, invasion, and metastasis.[68] The ability of CAFs to shape the extracellular stroma can form a barrier for drug or therapeutic immune cell penetration, thereby preventing drugs and immune cells from reaching tumour tissues and reducing the efficacy of tumour therapy. Therefore, tumour suppression by modulating CAFs or overcoming their barrier effect is a new tool in tumour therapy.[69–72]

The TME shows great diversity in immune cell composition across different types of cancers. Moreover, the environment surrounding tumour cells is characterised by chronic overexpression of inflammatory mediators, and the immune system has difficulty recognising and removing abnormal cells: immune cells do not respond to tumour cells. The primary immune populations (TAMs, MDSCs, neutrophils, DCs, T lymphocytes, and NK cells) play critical roles in the TME. It makes sense to target these populations to generate a positive cancer immune response and, thus, a therapeutic role. The acidic microenvironment surrounding tumour cells is an important feature of tumour ecosystems. The TME is primarily created by malignant cell metabolites, such as lactic acid, and other factors, such as irregular vascular morphology and hypoxic conditions. It has multiple effects on tumour cell survival, invasiveness, and drug resistance. Therapeutic strategies that target this feature should be developed and focus on releasing drugs that exploit the acidic environment to enhance their penetration within tumour cells and thus improve therapeutic efficacy.

In addition to these differential features, a common tumour, colon cancer, also has endogenous differences.[73] Because the production of H_2S selectively upregulates the expression of cystathione β-synthase, the H_2S content in the TME is much higher than that in normal tissues. This promotes colon cancer cell proliferation and blood vessel formation around the tumour tissue. The resulting blood vessels are highly permeable, promoting cancer cell invasion and spread.[74] Therefore, using biomaterials to consume H_2S differentially in colon cancer tumors has become a focus among researchers.

3. Design and applications of biomaterials with cancer cell-specific cytotoxicity

The physical and chemical properties of nanostructured materials depend on their sizes, structures, morphologies, and surface chemical states. In this section, we highlight strategies for designing various biomaterials with specific cytotoxicity by controlling their size, structure, morphology, surface modification, and external energy stimulation (Fig. 5 and Table 3).

3.1. Size

Nanoparticle penetration can be influenced by various factors, with particle size being significant. Particle size may affect nanoparticle penetration in several ways.

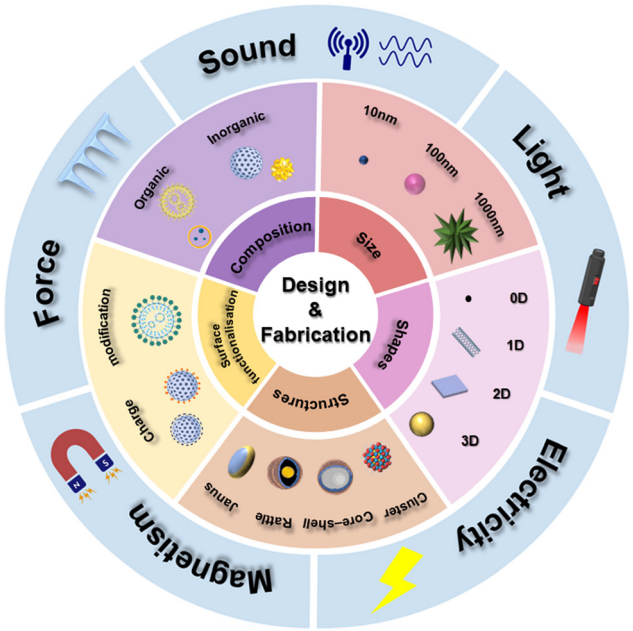

Fig. 5 Schematic application based on material design and synthesis using different ways to kill tumour cells differentially.

3.1.1. Barrier penetration. The nanoparticle sizes may limit their ability to penetrate physical barriers, such as the blood–brain barrier. Smaller nanoparticles may cross these barriers more quickly than larger ones. Therefore, nanoparticle size is a critical factor affecting their penetration capabilities, influencing interactions with biological barriers, cellular uptake mechanisms, biodistribution, and immune clearance.[75,76]

3.1.2. Devouring. Phagocytic mechanisms may affect nanomaterial particles of different sizes in different ways. Nanoparticle transport mechanisms, such as passive diffusion, active transport, and receptor-mediated transport, are size-dependent; for instance, smaller nanoparticles may more readily undergo passive diffusion across cellular membranes.[77,78] Smaller nanoparticles may undergo receptor-mediated endocytosis more quickly, allowing them to enter cells more efficiently than larger particles. This method can enhance interactions with biological barriers, facilitating penetration.[79,80]

3.1.3. Diffusion and metabolism. Smaller nanoparticles exhibit faster diffusion rates because of their larger Brownian motions when nanomaterials are engulfed and absorbed. As a result, they penetrate biological barriers more readily than larger particles. Meanwhile, nanoparticles of specific sizes may have affinities for certain organs or tissues, affecting their penetration into these areas.[81,82] Larger nanoparticles may be more readily recognised and cleared by the immune system, whereas smaller nanoparticles may evade immune recognition to a greater extent, allowing for prolonged circulation and enhanced penetration.[83]

Different tumour therapy nanoparticle sizes have their advantages and disadvantages. Small nanoparticles (1–100 nm) have enhanced penetration, improved circulation time, and high surface area but may suffer from potential

Table 3 Design of bioactive materials for specific cytotoxic treatment of oncological diseases

Material design	Characteristics	Composition	Mechanism	Therapy modalities	Ref.
Size	Size reduction	$PP_{IR780\text{-}ZMS}$	$Mn^{4+} \xrightarrow{H^+} Mn^{2+}$, $H_2O_2 \xrightarrow{Mn^{2+}} \bullet OH \uparrow$, $H_2O_2 \xrightarrow{CDT} ROS \uparrow$	PTT and CDT	88
		Au, DOX	PEG-PCRVP/AuNR@PDOX $\xrightarrow{pH}$ AuNR@PDOX $\xrightarrow{GSH}$ Au + DOX	Chemotherapy and PA	90
		HBPTK-Ce6@CPT	HBPTK-Ce6@CPT $\xrightarrow{NIR}$ CPT + Ce6	Chemotherapy	91
	Modulating size changes	TTVBI, DTVBI, and DTTVBI	DTTVBI $\xrightarrow{AIE}$ Gather	AIE, PDT, and PTT	92
Shapes	Nanodots	$MnFeO_4$-DCA NPs	$MnFeO_4$-DCA NPs → PDH ↑, Gycolysis $\xrightarrow{MnFeO_4\text{-}DCA\ NPs}$ ATP ↑ $\xrightarrow{MnFeO_4\text{-}DCA\ NPs}$ ADO ↓	PTT	101
		Au_{25}(S-TPP)$_{18}$	Mitochondrion $\xrightarrow{Au_{25}(S\text{-}TPP)_{18}}$ ROS	Chemotherapy and PA	102
	Nanowire	MoO_x (FMO)	$H_2O_2 \xrightarrow{Fe^{2+},Mo^{5+}} \bullet OH \uparrow$, GSH $\xrightarrow{Fe^{2+},Mo^{5+}}$ GSSH	PPT and CDT	104
		PEG-SS-CS-MAH/DOX NWs	PEG-SS-CS-MAH/DOX $\xrightarrow{pH}$ DOX	Chemotherapy	103
	Nanosheets	MnO_x@silicene-BSA	$M_nO_x + GSH \rightarrow Mn^{2+} + GSSG$, $M_nO_x + H^+ \rightarrow Mn^{2+} + H_2O$, $Mn^{2+} + H_2O_2 \xrightarrow{HCO_3^-} Mn^{x+} + \bullet OH$	PTT, MRI, and PAI	105
		LA@CoCuMo-LDH	LA@LDH $\xrightarrow{NIR}$ Cu^{2+} $\xrightarrow{H_2O_2}$ •OH $\xrightarrow{PDT/CDT}$ ROS ↑	PDT and CDT	106
		P-LDH-DOX	P-LDH-DOX $\xrightarrow{pH}$ DOX	Chemotherapy	107
	Nanoclusters	DEP@GdCuB	DEP@GdCuB + ATP → PTT ↑ + MRI ↑	PTT and MRI	108
	Nanoflowers	ZnO	ZnO $\xrightarrow{pierce}$ CTC	Physical stimulation	109
		Cu-TCPP-TCP	Cu-TCPP-TCP $\xrightarrow{NIR}$ PTT ↑	PTT	110
		Bac@MnO_2	$Mn^{2+} + H_2O_2 \rightarrow O_2$	CDT	111
Structures	Cluster structure core–shell structure	PDN	PDN $\xrightarrow{pH}$ DOX, PDN $\xrightarrow{GSH}$ NO	Chemotherapy and GT	112
		MIL-88-ICG@ZIF-8-DOX	$H_2O_2 \xrightarrow{MIL\text{-}88} O_2 + \bullet OH^-$	Chemotherapy, PTT, and PDT	113
		OxPt/SN38	OxP_t/SN38 $\xrightarrow{MIL\text{-}88}$ SN38	Chemotherapy and ICD	114
		Fn@CaP	CaP $\xrightarrow{dissolution}$ pH ↑	CDT	115 and 116
		UC NPs@$AgBiS_2$	$H_2O_2 \xrightarrow{UC\ NPs@AgBiS_2} \bullet OH$, $H_2O_2 \xrightarrow{UC\ NPs@AgBiS_2} O_2 \xrightarrow{UC\ NPs@AgBiS_2} {}^1O_2$	PTT and chemotherapy	117
		Au@BTO CSNSs	$H_2O \xrightarrow{Au@BTO\ CSNSs} \bullet OH$	PTT and CDT	118
		WP5 ⊃ TAPEG	WP5 ⊃ TAPEG $\xrightarrow{NIR}$ PTT	PTT	119
	Rattle structure	GNRs@PDA-BTS	GNRs@PDA-BTS $\xrightarrow{NIR}$ SO_2	PTT and CDT	120
	Janus structure	Cu_{2-x}Se-Au Janus NPs	$Cu^{2+} \xrightarrow{e^-} Cu^+$, $H_2O_2 \xrightarrow{Cu_{2-x}Se-Au} OH^- + \bullet OH$	PTT and CDT	121
		FeO@$mSiO_2$/Au-CAT	$Fe^{2+} + H_2O_2 \rightarrow Fe^{3+} + OH- + \bullet OH$	PDT and CDT	122

Table 3 (*continued*)

Material design	Characteristics	Composition	Mechanism	Therapy modalities	Ref.
Surface functionalisation	Surface modification	USP NPs	$\text{USP NPs} \xrightarrow{\text{NIR}} \text{SP} \uparrow, \quad \text{H}_2\text{O}_2 \xrightarrow{\text{SP}} {}^1\text{O}_2 \uparrow$	CDT and PTT	123
		Cu_2O@ΔSt	$\text{Cu}_2\text{O} \xrightarrow{\text{H}_2\text{S}} \text{CuS}$	PTT and CDT	124
		CCP@HP@M	$\text{H}_2\text{O}_2 \xrightarrow{\text{Pt}} \bullet\text{OH}, \quad \text{H}_2\text{O}_2 \xrightarrow{\text{Pt}} \text{O}_2 \xrightarrow{\text{SDT}} {}^1\text{O}_2, \quad \text{H}_2\text{O}_2 \xrightarrow{\text{HP}} \text{O}_2^{\bullet-}$	SDT	125
	Surface charge	HVDMs NPs	$\text{HVDMs} \xrightarrow{e^-} \text{pH} \uparrow + \text{DOX} \rightarrow \text{cell death}$	CDT	126
		R-NGs/DOX	$\text{R-NGs/DOX} \xrightarrow{\text{pH}} \text{DOX}$	Chemotherapy	127
External energy stimulation	Light-PDT	Ac-DEVDD-TPP	$\text{Ac-DEVDD-TPP} \xrightarrow{\text{NIR}} \text{D-TPP} \rightarrow {}^1\text{O}_2 \uparrow$	PDT and CDT	128
		GQD NT	$\text{GQD NT} \xrightarrow{\text{H}^+} \text{GQD NT} \uparrow \rightarrow \text{H}_2\text{O}_2 \xrightarrow{\text{NIR}} {}^1\text{O}_2 \rightarrow \text{ROS} \uparrow$	PDT and PTT	129
	PTT	UC NPs@$AgBiS_2$	$\text{H}_2\text{O}_2 \xrightarrow{\text{UC NPs@AgBiS}_2} \bullet\text{OH}, \quad \text{H}_2\text{O}_2 \xrightarrow{\text{UC NPs@AgBiS}_2} \text{O}_2 \xrightarrow{\text{UC NPs@AgBiS}_2} {}^1\text{O}_2$	PTT and chemotherapy	130
		D1	$\text{D1} \xrightarrow{\text{NIR}} \text{ROS}$	Chemotherapy and PTT	131
		(PCM + DOX)@Bi_2S_3	$\text{PD@BS} \xrightarrow{\text{NIR}} \text{DOX} \rightarrow \text{cell death} \uparrow$	PTT, CDT, and PA	132
		ZMS@PDA	$\text{Mn}^{4+} + \text{GSH} \rightarrow \text{Mn}^{2+} + \text{GSSG}, \quad \text{Mn}^{4+} + \text{H}^+ \rightarrow \text{Mn}^{2+} + \text{H}_2\text{O} \rightarrow \text{pH} \uparrow, \quad \text{Mn}^{2+} + \text{H}_2\text{O}_2 \xrightarrow{\text{HCO}_3^-} \text{Mn}^{4+} + \bullet\text{OH}$	PTT and CDT	133
		IRDNP-PLT, PDA@Dox NPs	$\text{PDA@Dox NPs} \xrightarrow{\text{NIR}} \text{DOX} \rightarrow \text{cell death} \uparrow$	CDT, PTT, and PDT	134
	Sound	$ZnSnO_3$:Nd	$\text{Zn}^{2+} \xrightarrow{\text{ETC}} \text{ATP} \downarrow, \quad \text{H}_2\text{O}_2 \xrightarrow{\text{ZnSnO}_3\text{:Nd}} \bullet\text{OH} + \text{O}_2^{\bullet-} + \text{O}_2 \xrightarrow{\text{ZnSnO}_3\text{:Nd}} {}^1\text{O}_2$	SDT and CDT	135
		5-exo-trig cyclisation and aminoglycoside antibiotics	$\text{Disulfide polymers} \xrightarrow{\text{US}} \text{thiols} \xrightarrow{\text{US}} \text{CPT}; \quad \text{phosphodiester RNA} \xrightarrow{\text{US}} \text{NeoB} + \text{Paromo}; \quad \text{PN} + \text{NN} + \text{VAN} \xrightarrow{\text{US}} \text{kill bacteria}$	Chemotherapy, MTT, and immunotherapy	136
	Magnetism	FVIOs-GO-CREKA	$\text{FVIOs-GO-CREKA} + \text{AMF} \xrightarrow{\text{MIT}} \text{ROS}$	MTT and immunotherapy	137
	Electricity	Tumour-treating fields	$\text{TNBC cells} \xrightarrow{\text{Tumor-treating fields+temozolomide}} \text{cell death}$	Electric field therapy	138
		TENG-CatSystem	$\text{TENG} \rightarrow \text{electric}, \quad \text{COF-CNT} + \text{1D ferriporphyrin} \xrightarrow{\text{Electric}} \text{ROS}$	Electric field therapy	139
		DOX@pPt NPs	$\text{pPt NPs} + \text{PEG} \rightarrow \text{pPT-PEG NPs}, \quad \text{H}_2\text{O}_2 \xrightarrow[\text{DOX@pPt}]{\text{Electric}} \bullet\text{H} + \bullet\text{OH}, \quad \text{DOX} \rightarrow \text{Apoptosis}$	EDT, and chemotherapy	140
	Force	CCPCA NPs	$\text{H}_2\text{O}_2 \xrightarrow{\text{CCPCA NPs}} \text{O}_2 \rightarrow \text{sO}_2 \uparrow, \quad \text{O}_2 + \text{PplX} \xrightarrow{\text{NIR}} {}^1\text{O}_2, \quad \text{GSH} + \text{Cu}^{2+} \xrightarrow{\text{NIR}} \text{GSSG}, \quad \text{H}_2\text{O}_2 \xrightarrow{\text{MN-CCPCA}} \text{O}_2 \xrightarrow{\text{NIR}} {}^1\text{O}_2$	CDT, and PDT	141

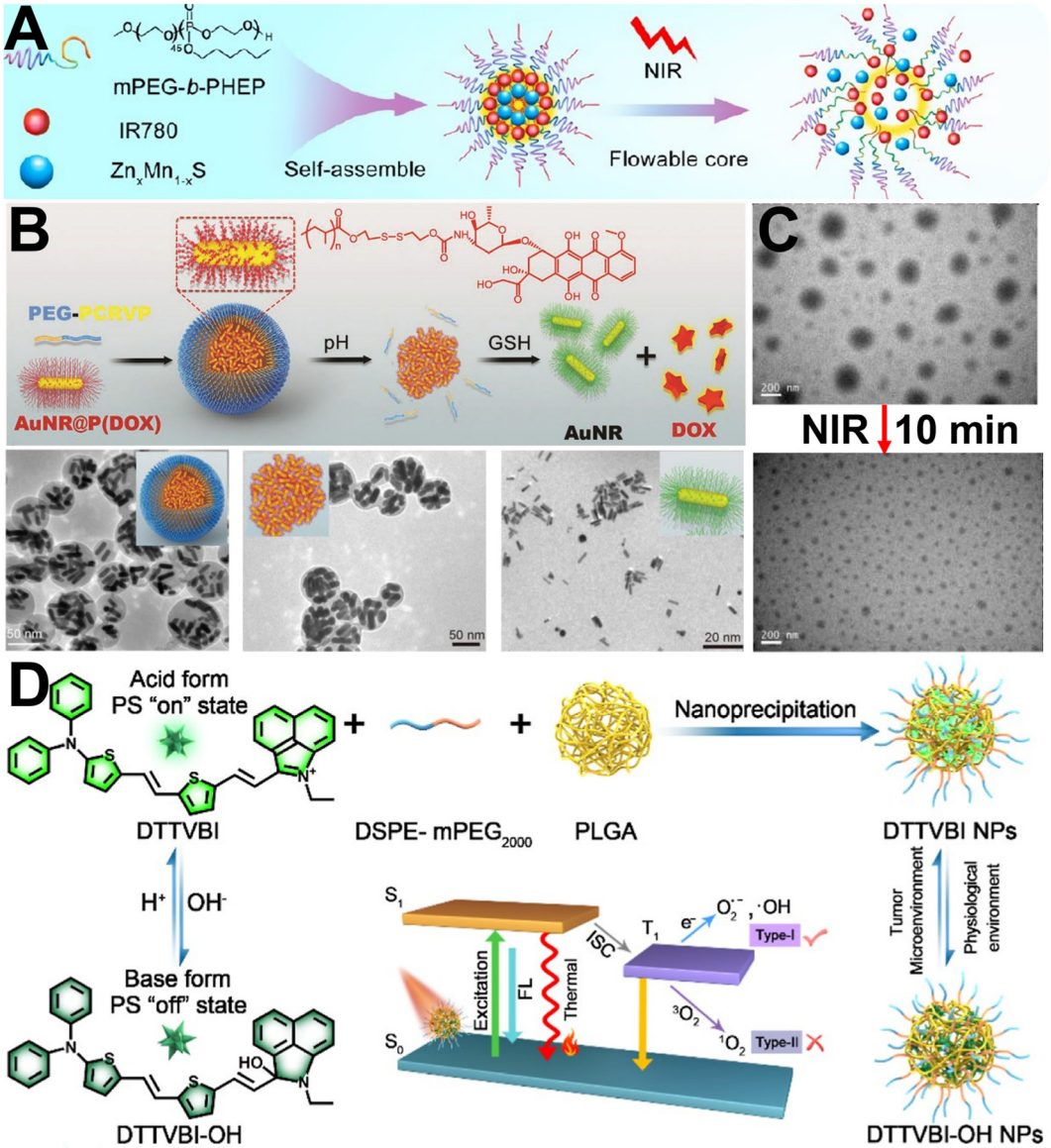

Fig. 6 Specific killing of tumour cells based on the biomaterial size change: (A) PPIR780-ZMS enhances CDT through photothermal release of nanoparticles and photosensitisers. Reproduced with permission from ref. 88. Copyright 2022, American Chemical Society; (B) PEG-PCRVP/AuNR@PDOX pH- and GSH dual-responsive size-change-released drug-enhanced chemotherapy. Reproduced with permission from ref. 90. Copyright 2019, Wiley-VCH; (C) HBPTK-Ce6@CPT laser intermittently affects size-change-enhanced drug-penetration therapy. Reproduced with permission from ref. 91. Copyright 2019, Elsevier Ltd; and (D) DTTVBI-OH NPs enhance therapeutic effectiveness through AIE. Reproduced with permission from ref. 92. Copyright 2023, American Chemical Society.

toxicity, limited payload capacity, and rapid clearance. Medium-sized nanoparticles (100–200 nm) can utilise the EPR effect efficiently, balance penetration and retention, and offer flexible surface functionalisation but may have moderate penetration and susceptibility to immune recognition. Large nanoparticles (>200 nm) exhibit enhanced retention and stability and high multifunctionality but may have limited penetration, may be susceptible to immune clearance, and often require complex synthesis and characterisation.[80]

The penetration depth of NPs within tumours is statistically correlated with their size. Intratumour accumulation requires nanoparticle sizes below 200 nm.[84,85] Within that range, larger sizes (~60–100 nm) can improve *in vivo* pharmacokinetics, prolong blood circulation, and reduce reticuloendothelial system (RES) clearance relative to other sizes; however, their poor intratumour penetration and distribution remain a challenge.[86] In contrast, ultrasmall sizes of less than 10 nm actively enhance tumour infiltration, but their quick elimination results in a reduced half-life in the bloodstream and restricted tumour accumulation.[87] Hence, optimal NPs must possess a larger nanoscale dimension (~100 nm) and a stable structure for blood circulation that can swiftly transform into a smaller dimension (~10 nm) to facilitate deeper tumour penetration and enhance drug aggregation.

Li *et al.* encapsulated the photosensitiser (PS) IR780 and zinc manganese sulphide (ZMS) NPs in an amphiphilic poly(ethylene glycol)-poly(2-hexyloxy-2-yloxy-1,3,2-dioxaphosphinane) (mPEG-*b*-PHEP) polymer (PPIR780-ZMS) (Fig. 6A).[88] This strategy promoted the release of small ZMS particles through the photothermal effect of IR780 in the presence of an 808 nm laser, thereby enhancing CDT and immunotherapy and inhibiting tumour growth and lung metastasis. The use of thermoresponsive amphiphilic polymers achieved size variation for the targeted, quantitative release of ZMS in tumour cells and avoided the high toxicity of inorganic nanomaterials toward normal cells, achieving the goal of differential toxicity therapy. Hua *et al.* designed a multistage, responsive, clustered nanosystem to systematically resolve multiple tumour biobarrier conflicts between the EPR effect and spatially homogeneous NP penetration by modulating nanoparticle size changes.[89] Nanosystems with ideal diameters (~50 nm initial size) favored long blood circulation and a tendency to hyperpermeability through tumour vascular gaps, which could be efficiently clustered around tumour tissues using the EPR effect. The hydrogen (pH)-sensitive nanoparticle agglomerates formed large aggregates (~1000 nm) in the tumour in the TME and showed good tumour retention. Subsequent photothermal treatment dispersed the aggregates into ultrasmall Au nanoclusters (~5 nm), which improved their tumour penetration ability and enhanced the radiotherapeutic effect of the radiosensitiser.

Jin *et al.* made another attempt to take advantage of the excellent photothermal properties of Au (Fig. 6B).[90] Poly(ethylene glycol)-*b*-((2,5-bis[(4-carboxylic acid piperidinylamino)thiophenyl]-*co*-4-vinylpyridine (PEG-PCRVP) encapsulated AuNRs (iophenyl]-,were grafted with poly(adriamycin)AuNR@PDO) to form a dual pH- and reduction-responsive nanoplatform (PEG-PCRVP/AuNR@PDOX). Initially, the NPs were approximately 70 nm in size at physiological pH levels. They had a longer blood circulation time, leading to a higher efficiency of tumour accumulation through the EPR effect. As the aggregated NPs entered the tumor space, the loss of the AuNR@PDOX cluster PEG-PCRVP shells due to the acidic environment caused the clusters to disintegrate into individual AuNR@PDOX NPs. Finally, AuNR@PDOX NPs ~12 nm in size penetrated the solid tumour regions and released doxorubicin (DOX) to kill cancer cells, resulting in an overall differential size alteration to enhance the killing effect of the chemotherapy.

Similar work was done by Liu *et al.* (Fig. 6C).[91] amphiphilic hyperbranched polyphosphate (HBPTK-Ce6) containing thione units and the PS was self-assembled and then encapsulated with camptothecin (CPT, a hypoxia-inducible factor-1α (HIF-1α) inhibitor) to form HBPTK-Ce6@CPT. After a 660 nm laser irradiation interval, Chlorin e6 (Ce6) in the HBPTK-Ce6 NPs efficiently generates ROS to kill cancer cells. At the same time, thione unit cleavage sequentially reduced the NP sizes, facilitating faster diffusion and more effective tumour penetration of NPs—an instance of programmable CPT.

In addition to reducing the nanomaterial size to enhance penetration, aggregation of nanomaterials to larger sizes can also achieve the specific killing of tumour cells. For example, aggregation-induced luminescence (AIE) is based on the principle that individual molecules do not emit light because they release energy through single-chain rotation. Molecule aggregation restricts individual molecule movements, enabling more energy to be emitted as radiation to produce visible luminescence.[93,94] Taking advantage of this property, Xiao *et al.* constructed NPs TTVBI, DTVBI, and DTTVBI that possessed near-infrared (NIR)-II AIE properties, aggregation caused quenching (ACQ) performance, high ROS-generation capacity, and photothermal conversion efficiency (Fig. 6D).[92] For synergistic type I photodynamic therapy (PDT)/photothermal therapy (PTT) of a colon cancer patient-derived xenograft model, the DTTVBI NPs exhibited excellent pH reversibility, NIR-II FLI tumour imaging capability, and a significant tumour-killing effect. The nanomaterial size change produced deeper penetration of dramatic lesions and enhanced the therapeutic process, reflecting the concept of differential toxicity in the nanomaterial design process.

3.2. Shapes

Shapes determine properties, and within the field of biomedical engineering, applications can be broadly classified into four main categories: points (dots (0D)), lines (one-dimensional (1D)), surfaces (two-dimensional (2D)), and bodies (three-dimensional (3D)). The shapes of nanomedicines can significantly affect their tumour therapy effectiveness. (1) Enhanced targeting: nanoparticles with specific shapes exhibit enhanced targeting. For example, rod-shaped or elongated nanoparticles can extravasate from leaky tumour blood vessels and accumulate within the tumour interstitium *via* the EPR effect. This targeted accumulation can improve drug delivery to tumour cells while minimising off-target effects.[95] (2) Cellular uptake: nanoparticle shapes can influence their cell interactions and subsequent internalisation. Specific shapes can facilitate receptor-mediated endocytosis or other uptake mechanisms, leading to increased cellular uptake of therapeutic agents. This enhanced internalisation can improve tumour therapy efficacy by delivering a higher drug concentration to cancer cells.[96] (3) Intracellular trafficking: different nanoparticle shapes can affect their intracellular trafficking pathways after cellular uptake. This can affect the subcellular localisation of therapeutic agents and their interactions with intracellular targets, influencing tumour therapy efficacy.[97] (4) Interaction with biological barriers: nanoparticle shapes can affect their interactions with biological barriers, such as the extracellular matrix, cellular membranes, and biological fluids. Particular shapes may exhibit improved penetration through biological barriers, allowing for deeper tumour penetration and better distribution within the TME.[98] (5) Stability and circulation time: nanoparticle shapes can influence their stability under physiological conditions and circulation time in the bloodstream. Shapes that minimise interactions with serum proteins and immune cells may exhibit prolonged circulation, allowing for increased accumulation within tumours and improved therapeutic efficacy.[99] (6) Multifunctionality: certain nanoparticle shapes can be engineered to incorporate multiple functionalities, such as targeting ligands, imaging agents, and therapeutic payloads, onto their surfaces. This

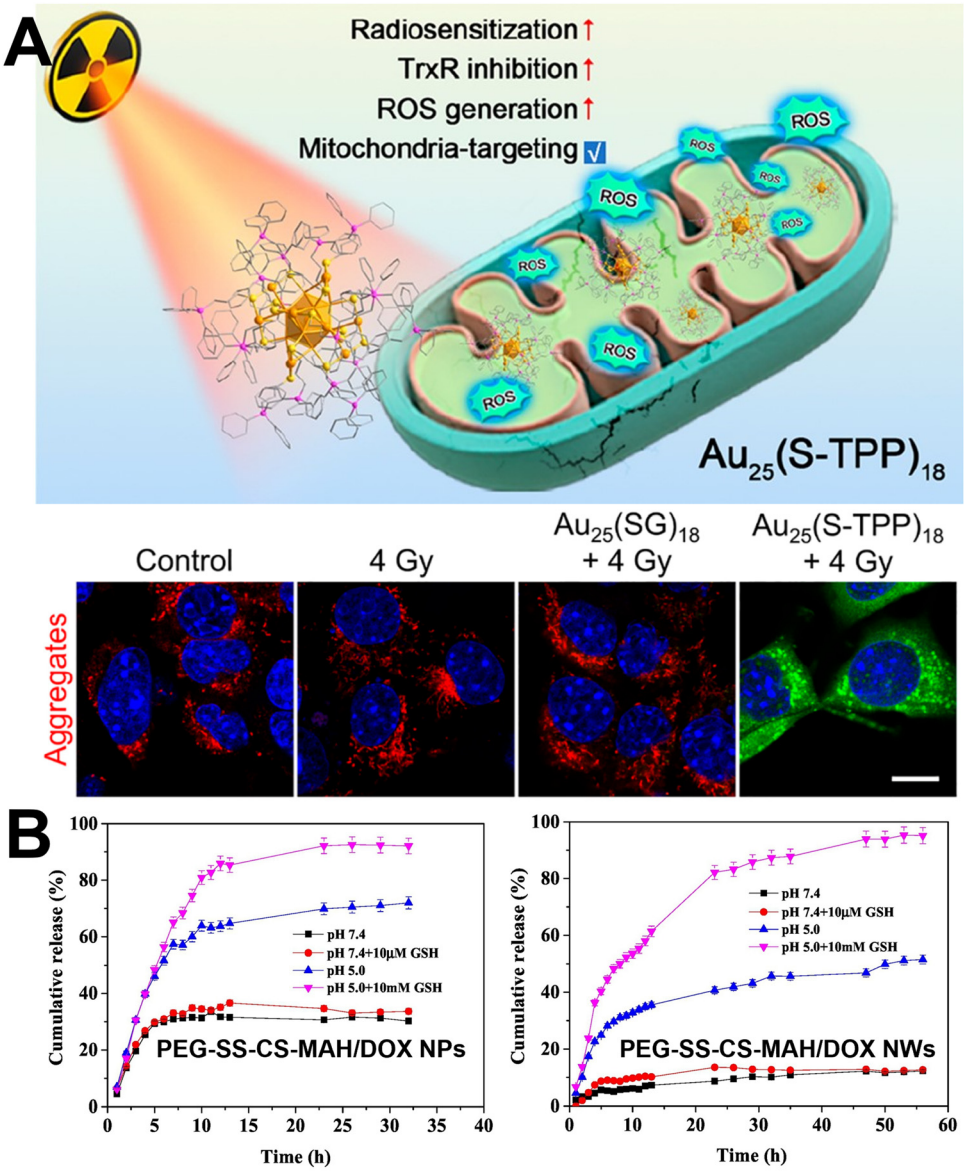

Fig. 7 Biomaterial shape-based design for 0–1D differential treatment of tumours: (A) Au_{25} (S-TPP)$_{18}$ nanoclusters enter mitochondria to produce ROS and inhibit TrxR. Reproduced with permission from ref. 102. Copyright 2023, American Chemical Society. (B) PEG-SS-CS-MAH/DOX NWs enhance DOX release. Reproduced with permission from ref. 103. Copyright 2022, Elsevier Ltd.

multifunctionality can improve tumour therapy specificity and efficacy by enabling targeted delivery, real-time imaging, and combination therapy approaches.[100] Overall, the shape of nanomedicines plays a crucial role in determining their effectiveness in tumour therapy by influencing multiple aspects of their pharmacokinetics, biodistribution, cellular uptake, intracellular trafficking, and TME interactions. The relationship between the shape design and properties is briefly described below.

3.2.1. 0D. Generally, 0D is considered to be a nanodot smaller than 10 nm, which provides good tumour penetration and can penetrate deep into intracellular organelles, such as mitochondria. For example, Dai *et al.* successfully synthesised a nanoparticle composed of manganese ferrite ($MnFe_2O_4$) and dichloroacetic acid (DCA) smaller than 6 nm.[101] This innovative nanoparticle was developed to modulate tumour glucose metabolism and ATP catabolism, reversing the immunosuppressive microenvironment typically observed in tumours. By effectively infiltrating the mitochondria for oxygen provision, enhancing DCA bioactivity, and regulating glucose metabolism, the ultramicro $MnFe_2O_4$-DCA NPs achieved a remarkable 100-fold decrease in lactate production compared with free DCA. In addition, to further improve mitochondrial entry efficiency, Hua *et al.* designed atomically precise Au_{25}(S-TPP)$_{18}$ clusters (TPP-SNa = sodium 3-(triphenylphosphine)propane-1-thiol bromide) (Fig. 7A), which by ligand design showed mitochondrial targeting ability and water solubility for enhanced radioimmunotherapy.[102] Compared to the Au_{25}(S-TPP)$_{18}$

clusters (SG = glutathione), Au_{25}(S-TPP)$_{18}$ exhibited higher radiosensitisation efficiency due to its mitochondrial targeting ability, higher ROS production capacity, and significant inhibition of TrxR.

3.2.2. 1D. 1D is a line, and in biological applications, common nanowires include molybdenum oxide (MoOx), silicon, calcium silicate, and chitosan, which exhibit high biosafety and rapid degradation in organisms. Chen *et al.* injected Fe-doped MoOx (FMO) ultrafine NPs *in situ* at the tumour site. They used high photothermal conversion-efficient PTT to enhance CDT by synergistic redox reactions of PTT with Fe and Mn sources.[104] The nanowire itself degraded rapidly in the acidic environment with high biosafety, achieving the purpose of differential tumour cell killing. Nanowires can be loaded with more drugs than conventional NPs. Xie *et al.* attempted to load DOX with polyethylene glycol (PEG)- and maleic anhydride (MAH)-modified chitosan (PEG-SS-CS-MAH) for pH/hypoxia dual-triggered DOX delivery (Fig. 7B).[103] Compared with PEG-SS-CS-MAH/DOX NPs, PEG-SS-CS-MAH/DOX NWs had higher drug-loading capacity, better pH/hypoxia dual-triggered DOX release, and higher cytotoxicity; the improved drug delivery could be differentially harmful to tumour cells.

3.2.3. 2D. Nanosheets have the advantage of a large surface area, which can be used to enhance their therapeutic effect in oncological diseases by allowing nanomaterials to absorb more physical energy, improve reaction efficiency, and increase drug loading. Duan *et al.* used 2D silicon nanosheets (SNSs) as substrates and grew highly dispersed manganese oxide (MnO_x) NPs on the surface of SNSs *in situ*.[105] The prepared MnOx@silicene-BSA composite nanosheets were used as multifunctional therapeutic nanoplatforms. Their large surface area has been used to absorb more physical energy to power multifunctional therapy that combines magnetic resonance imaging (MRI), photoacoustic imaging (PAI), photonic thermotherapy, and nanocatalytic therapy.

Yang *et al.* utilised *Lactobacillus acidophilus* with 2D CoCuMo-LDH nanosheets to execute targeted and precise NIR-II PDT for tumour treatment.[106] The nanosheets underwent amorphisation under TME influence when exposed to 1270 nm laser radiation. This process significantly bolstered the ability of the nanosheets to generate ROS, with their activity being approximately 42.8 times greater than that of unamorphised CoCuMo-LDH nanosheets. Additionally, the amorphous CoCuMo-LDH nanosheets displayed a relatively single-linear oxygen ($^1O_2$) quantum yield of 1.06, and their high catalytic activity enabled a new level of tumour cell-killing.

Fewer layers of lactate dehydrogenase (LDH) nanosheets were formed by the surface coupling of poly(oligo(ethylene glycol) methyl ether acrylate)-*block*-poly(monoacryloxyphosphoric acid ethyl ester) by Zhang *et al.* (Fig. 8A).[107] The synthesised P-LDH nanosheets exhibited excellent colloidal stability and an ultrahigh drug loading (734% using DOX as a model drug). Prolonged blood circulation enhanced the cellular uptake of the ultrahigh drug-loaded P-LDH nanosheets, which could release the drug in response to pH.

3.2.4. 3D. 3D implies spatial three-dimensionality, and 3D nanomaterials are distinguished by a wide variety of structures, such as nanoclusters, nanoflowers, nanoscaffolds, and engineered nanobacteria. These different structures enable different roles for these materials in treating oncological diseases. For example, nanoclusters can deeply penetrate tumour tissues because they are smaller. Zhou *et al.* prepared Gd^{3+} and Cu-loaded bovine serum albumin (BSA) NPs (GdCuB), after which phenylboronic acid and ethylenediamine-modified dextrin (DEP) were synthesised as charge-switchable polycationic carriers. GdCuB was encapsulated in DEP to form DEP/GdCuB clusters.[108] The properties of the synthesised nanoclusters were such that when the nanoclusters were in blood circulation, the relatively large size of DEP/GdCuB prolonged the half-life of GdCuB, which promoted tumour accumulation and impaired the *T*1-weighted MRI effect of GdCuB. When accumulated at the tumour site, extracellular ATP triggered the release of GdCuB, promoting deep cluster penetration and activating MRI and PTT. The presence of nanoflowers is more specific, and some nanoflower synthesis processes involve nanosheet preparation. Therefore, nanoflowers also possess most of the desirable properties of nanosheets. Another property of zinc oxide (ZnO) nanoflowers was discovered by Li *et al.* (Fig. 8B), who captured and killed approximately 90% of circulating tumour cells (CTCs) *in vitro* by coating ZnO nanoflowers (ZNFs) on medical needles.[109] The nanoflower structure has a larger surface area than a vertical nanowire and a 3D extrusion capability, making CTCs easier to puncture.

Nanoscaffolds, as the name suggests, support the missing position; they are generally applied to the vacant site after tumour resection, and the properties possessed by nanoscaffolds should not only inhibit the growth of tumours but also promote wound healing and regeneration of normal tissue cells in the wound site. Therefore, Dang *et al.* used 3D-printing technology and *in situ* growth to prepare a β-tricalcium phosphate (TCP) (Cu-TCPP-TCP) scaffold structured at the interface of Cu-TCPP nanosheets.[110] Because Cu has good photothermal properties, it can inhibit *in situ* residual tumour cell growth and slow recurrence. The nanoscaffolds were implanted into human bone marrow stromal cells (HBMSCs) and human umbilical vein endothelial cells (HUVECs); they significantly stimulated gene expression related to osteogenic differentiation in HBMSCs and angiogenic differentiation in HUVECs, effectively promoting bone regeneration.

The preparation of nanoengineered bacteria involves designing products according to their intended purpose. The desired products can be designed by taking advantage of the tumour site characteristics, such as hypoxia, microacidity, high lactic acid, and high GSH. For example, taking advantage of excess lactate at the tumour site due to hypoxia, Chen *et al.* constructed a lactate-fuelled biomixture (Bac@MnO_2) using *Shewanella oneidensis* MR-1 (*S. oneidensis* MR-1) externally modified with manganese dioxide (MnO_2). *S. oneidensis* MR-1 nanoflowers targeted lactate consumption through hypoxic properties to starve tumour cells.[111] In addition, decorated MnO_2 nanoflowers catalysed endogenous H_2O_2 conversion to

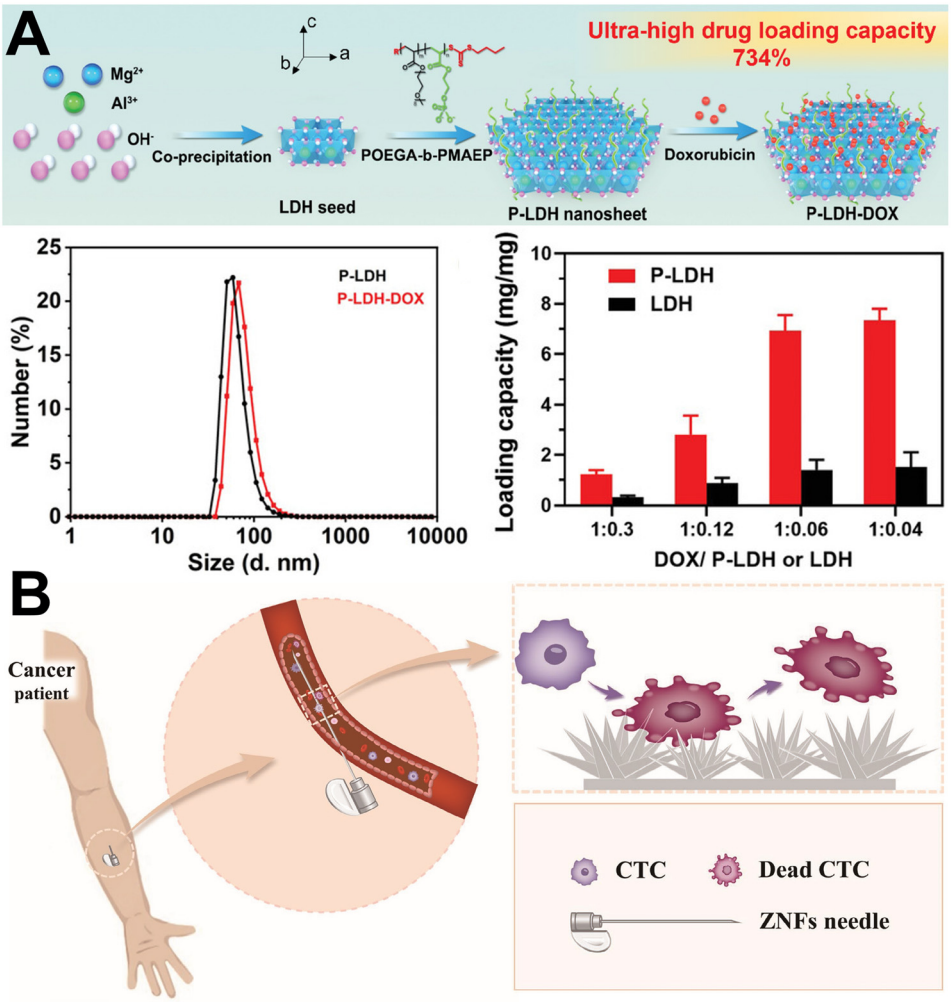

Fig. 8 Biomaterial shape-based design for 2-3D differential treatment of tumours: (A) P-LDH-DOX nanosheets enhance DOX loading. Reproduced with permission from ref. 107. Copyright 2022, Wiley-VCH. (B) ZnO nanoflowers effectively puncture CTCs. Reproduced with permission from ref. 109. Copyright 2023, Springer Nature.

produce oxygen (O_2) and downregulated HIF-1α to inhibit lactate production, ultimately achieving differential killing of tumour cells.

3.3. Structures

Particle shape affects *in vivo* distribution and cellular internalisation, with rod-shaped nanoparticles having a longer residence time in the gastrointestinal tract than spherical nanoparticles.[142–144] The elongated particles have an advantage in targeting the endothelium and display higher specific adhesion and higher endothelium affinity and selectivity.[145] Other nonspherical particles, especially discoidal particles, have a tumour accumulation rate on the micron and nanometre scales five times that of the same-sized spherical particles.[146] Thus, different shapes have different functions, providing opportunities for specific toxicity. Cluster, core/shell, rattle, and Janus structures offer unique opportunities to improve nanomedicine effectiveness in tumour therapy through enhanced drug delivery, targeting specificity, controlled release, and imaging capabilities. These nanostructures can be tailored to address specific challenges associated with cancer treatment, such as drug resistance, tumour heterogeneity, and off-target effects, thereby advancing the development of more efficient and personalised cancer therapies.

3.3.1. Cluster structures. Clusters are macroscopic nanostructures (NSs) in which multiple nanosystems are stacked. They are generally used in biomedical applications for tumour therapy *via* endogenous stimulation, thereby changing their size to promote tumour penetration. For example, Wang *et al.* designed a tumour acidity- and bioorthogonal chemistry-mediated *in situ* size-transformed cluster nanosystem for enhanced tumour penetration and accumulation of drugs (Fig. 9A).[112] The nanosystem utilises an oncolytic acid-reactive group, poly(2-azacyclohexane ethyl methacrylate), with a fast reaction rate and efficient bioorthogonal click chemistry to form large aggregates in the tumour tissue for enhanced accumulation and retention. Subsequently, another slow-reacting maleic acid amide tumour-acid-reactive group was

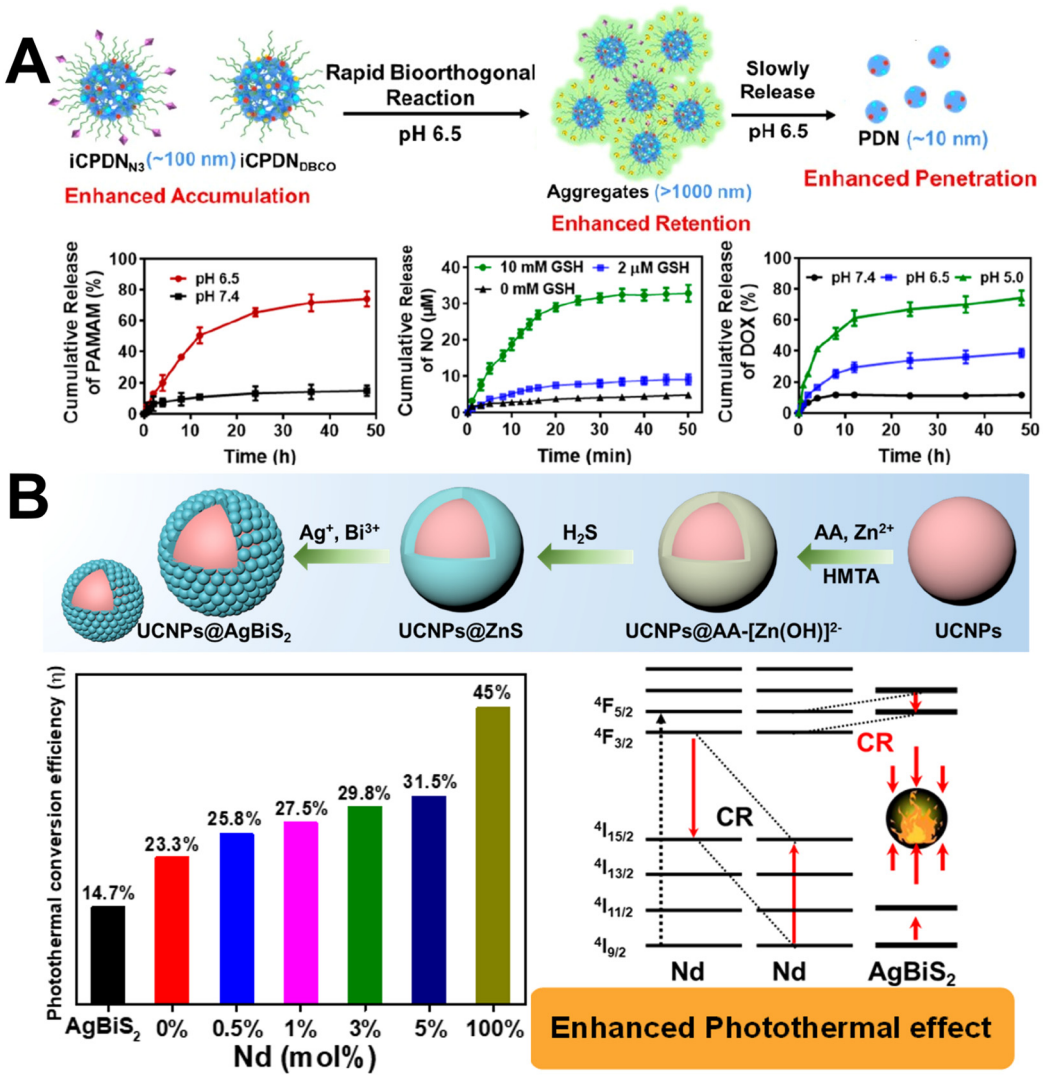

Fig. 9 Specific tumour killing based on nanostructures: (A) PDN nanoclusters overcome tumour hypoxia. Reproduced with permission from ref. 112. Copyright 2022, American Chemical Society. (B) UC NPs@AgBiS$_2$ core/shell structure enhances the photothermal effect and kills tumour cells. Reproduced with permission from ref. 117. Copyright 2022, Elsevier Ltd. (C) GNRs@PDA-BTS photothermal/phosphate triggered-gas therapy. Reproduced with permission from ref. 120. Copyright 2020, Elsevier Ltd. (D) Janus nanocatalytic robotics with FeO@mSiO$_2$/Au-CAT enhances tumour penetration and therapy. Reproduced with permission from ref. 122. Copyright 2023, American Chemical Society.

cleaved. This allowed the aggregates to dissociate slowly into ultrasmall NPs with improved tumour penetration to deliver DOX and nitric oxide to hypoxic tumour tissues.

3.3.2. Core/shell structures. The core/shell structure is a nanoscale ordered-assembly structure formed by one nanomaterial encapsulating another nanomaterial through chemical bonding or other forces. The core encapsulates therapeutic payloads, whereas the shell provides protection, controlled release, and targeted functionalities. This design enables efficient drug delivery to tumour sites, controlled release in response to specific stimuli (such as pH, enzymes, or temperature), and targeted accumulation within cancer cells, minimising systemic toxicity and maximising therapeutic efficacy. The core/shell structure utilises the properties of both internal and external materials. It allows them to complement each other's deficiencies, an important research direction for morphology-determined properties.

First, the core/shell structure provides a strategy for drug release. Wu *et al.* designed a core/shell metal–organic framework drug release system.[113] This system exhibited the distinctive characteristics of both materials and offered two distinct functional regions for simultaneous drug delivery. Both PS indocyanine green (ICG) and the chemotherapeutic drug DOX were systematically incorporated within the nanopores of the MIL-88 core and zeolitic imidazolate framework-8 (ZIF-8) shell, facilitating the fabrication of a synergistic nanoplatform that combined photothermal, photodynamic, and chemotherapeutic effects. In addition to direct drug release, Jiang *et al.* reported a two-stage core/shell structure release strategy to minimise nanomedicine haematological toxicity caused by

prolonged blood circulation.[114] The structure was based on a hydrophilic oxaliplatin (OxPt) prodrug coordination polymer as the core and a hydrophobic cholesterol-coupled SN38 prodrug (Chol-SN38) lipid as the shell. In particular, Chol-SN38 releases 7-ethyl-10-hydroxycamptothecin (SN38) in two phases, esterase-catalysed acetal bond cleavage and acid-mediated hydrolysis of the trimethylsilyl moiety, thereby decreasing blood exposure and increasing tumour exposure. pH-responsive, inorganic nanoshells can also alter drug release properties and pharmacokinetics. For example, Xu *et al.* and Wang *et al.* used CaP as a nanoparticle shell to coat DOX and ferritin (Fn), respectively, which improved pharmacokinetics and drug accumulation, thereby enhancing the inhibition of tumour growth.[115,116]

The composition design inside and outside the core/shell structure can be used to improve the properties. Chu *et al.* grew $AgBiS_2$ epitaxially on the surface of upconversion NPs (UCNPs) and successfully prepared UCNPs@$AgBiS_2$ core/shell NPs (Fig. 9B).[117] They varied the Nd-ion doping concentration in the UCNPs to modulate the cross-relaxation between Nd ions and $AgBiS_2$ and obtained higher photothermal and ROS-generation efficiencies. Chang *et al.* designed new plasma-pyroelectric Au@barium titanate (BTO) core/shell (CS) NSs to generate temperature-mediated O_2-independent PDT for hypoxic tumour therapy.[118] Laser irradiation (808 nm) excited the Au core, and the resulting heat transferred to the pyroelectric BTO shell. The increased temperature decreased spontaneous BTO polarisation, releasing a large number of holes from the BTO surface and promoting the formation of highly reactive oxygen radicals ($^{\bullet}OH$) in an O_2-independent manner. In addition to direct interactions, Wang *et al.* constructed core/shell nanostructures induced by host–guest interactions between water-soluble columnar aromatic hydrocarbons and poly(ethylene glycol)-modified aniline tetramer, which conferred a size-switchable property on the core/shell nanostructures through pH responsiveness.[119] The dual mechanism of structural switching and coupling of the core/shell nanostructures in acidic microenvironments modulates the extension, the inclusions in the hydrophobic cavities, and the density distribution in the core/shell structural components, which significantly enhances the absorption in the NIR-II region and consequently improves the photothermal conversion efficiency.

3.3.3. Rattle structures. The rattle-shell structure is called the yolk–shell structure. Compared with the core/shell structure, it contains a void layer with a specific drug-loading performance and can completely expose the active sites of internal and external substances. The void layer between the ''yolk'' and shell provides a larger space for the catalytic reaction and ensures a high substrate and product diffusion rate. Rattle nanoparticles can be loaded with therapeutic agents, contrast agents, or imaging probes within their hollow core, allowing simultaneous drug delivery and real-time imaging of tumour sites. The shell can be tailored to respond to specific stimuli or target tumour biomarkers, facilitating controlled drug release and enhanced accumulation within cancer cells. For example, Lu *et al.* removed the silicon dioxide (SiO_2) between the Au nanorod core and the outermost polydopamine (PDA) shell by HF etching. They loaded the sulfur dioxide (SO_2) precursor to form a highly drug-loaded rattling structure (Fig. 10A).[120] The release of SO_2 gas can be precisely controlled by photothermal stimulation and pH changes, realising the ''complicity'' between ''inner'' gas therapy and ''outer'' PTT. In addition, Liang *et al.* constructed a rattle structure with Fe as the nucleus and magnetite as the shell, stabilizing the active sites of Fe(0) in the nucleus and controlling the release of Fe(0) into the TME to enhance cancer treatment.[147]

3.3.4. Janus structures. Janus nanostructures have two distinguishable, dissimilar surfaces or components. The advantage of this structure is that, on the one hand, it can promote electron distribution, while on the other, its different surfaces have different reaction properties, resulting in an inert side and an active side that can react with the substrate, produce different states, and exhibit motility, that is nanomotor functionality. For example, Janus nanoparticles can be engineered to equip one hemisphere for drug loading and release, whereas the other can be functionalised with targeting ligands or imaging agents. This design enables selective tumour cell targeting, real-time drug delivery and distribution imaging, and controlled release in response to external stimuli or TME cues. This leads to enhanced therapeutic efficacy and reduced side effects. For example, Wang *et al.* constructed $Cu_{2-x}Se$–Au Janus NPs, where the amorphous nature of $Cu_{2-x}Se$ and the catalytic impact of Au favored $^{\bullet}OH$ generation, while the light-induced electron–hole separation of the Janus NPs generated additional $^{\bullet}OH$.[121] Sun *et al.* designed a core of ferrous oxide (FeO) and mesoporous SiO_2 ($mSiO_2$), with a part of the surface as the Au shell and another part of bare $mSiO_2$ loaded with CAT enzyme to form FeO@$mSiO_2$/Au-CAT Janus NPs (Fig. 10B).[122] Utilising the unique Janus structure, these Janus NPs exhibited active motility in H_2O_2 solution, and their migration in tumour tissues could be tracked in real time by noninvasive MRI. These self-containing Janus NPs penetrated deeper into the tumour and enhanced oncology therapy after intratumoural injection compared with passive NPs.

3.4. Surface functionalisation

3.4.1. Surface modification. The primary purpose of biomaterial surface modification is to enhance biosafety in tumour disease treatment by achieving more specific killing of tumour cells. Surface modifications include polymer, bacterial, and tumour cell membrane alterations.

The essential characteristic of a polymer surface is that it can be designed and synthesised to possess required properties, such as amphiphilicity and thermal response. Commonly used polymer modifications must consider two critical properties: hydrophilicity and hydrophobicity. For example, hydrophilic PEG can prevent the adhesion of plasma proteins, which increases the circulation time of drugs in the body during injectable therapy. Hydrophobicity can encapsulate therapeutic drugs or biomaterials to enhance drug delivery. Chu *et al.* used ultrasound to incorporate a fluoroquinolone antibiotic drug (sparfloxacin (SP)) and UCNPs into the thermally sensitive,

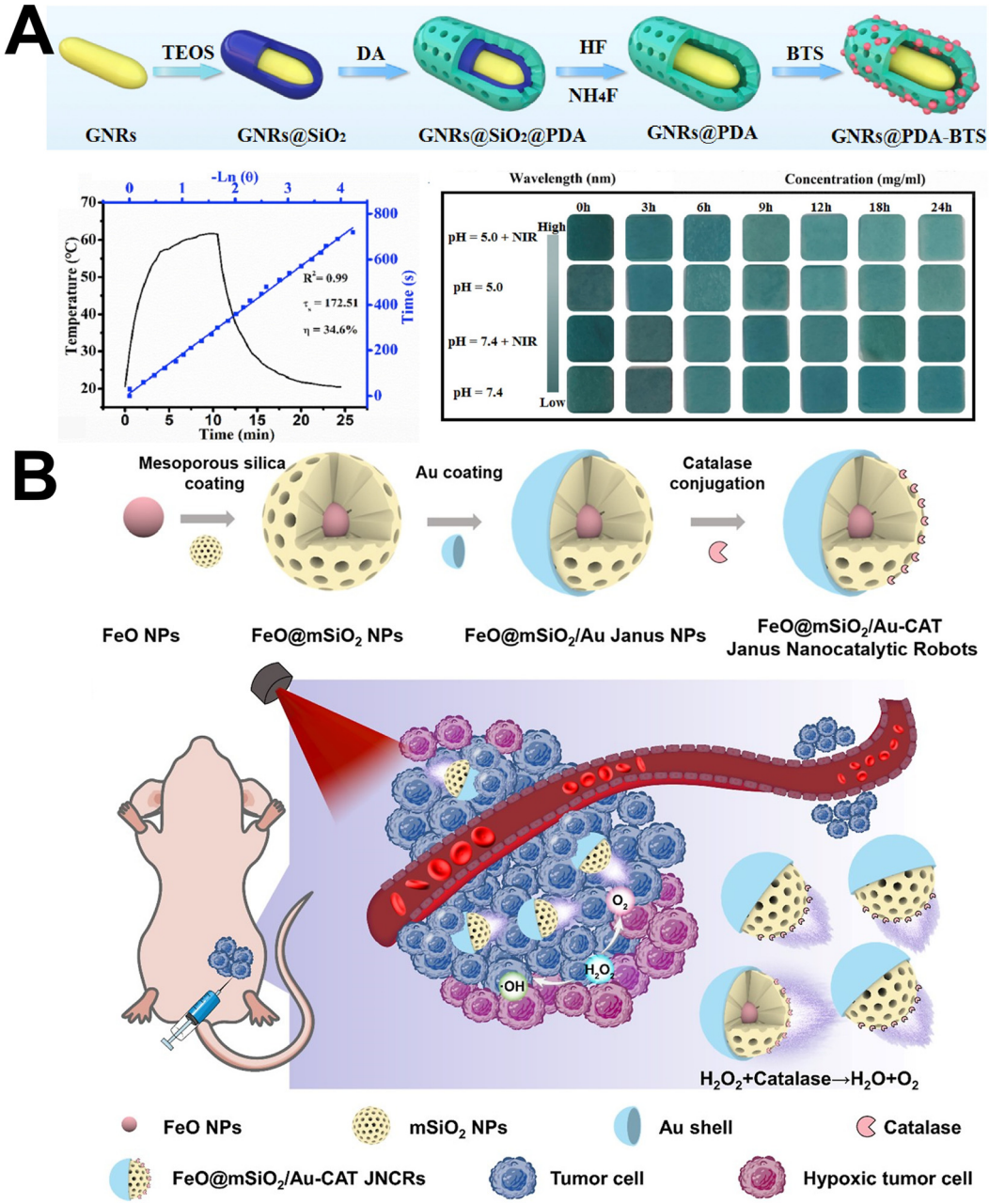

Fig. 10 Specific tumour killing based on nanostructures: (A) GNRs@PDA-BTS photothermal/phosphate triggered-gas therapy. Reproduced with permission from ref. 120. Copyright 2020, Elsevier Ltd. (B) Janus nanocatalytic robotics with FeO@mSiO$_2$/Au-CAT enhances tumour penetration and therapy. Reproduced with permission from ref. 122. Copyright 2023, American Chemical Society.

amphiphilic polymer mPEG-*b*-PHEP to treat *in situ* breast cancer in mice (Fig. 11A).[123] The specific killing of tumour cells was achieved using laser irradiation, heat release of SP, and ROS generation to enhance chemotherapy.

Although artificially prepared macromolecules can have specific therapeutic effects, the biocompatibility and safety of natural organisms can be enhanced by treatments. Organism examples include bacteria, which are ubiquitous in life, and living cell membranes. Bacteria are often thought of as disease carriers that are difficult to treat; however, with continuous exploitation, bacteria such as those found in cheese, yoghurt, and wine are gradually coming into public view. The unique physicochemical characteristics of some bacteria (capacity for anoxic targeting, gas targeting, acidic targeting, and so on) provide possibilities for treating diseases.[148–152]

When the anaerobic characteristics of *Salmonella* bacteria (ΔS_t) were used to target and colonise anoxic tumour sites, the H_2S gas produced sulphurised cuprous oxide (Cu_2O) to copper sulphide to enhance PTT, and the acidic TME released Cu^+ that promoted tumour fenestration (Fig. 11B).[124] The Cu^+ released

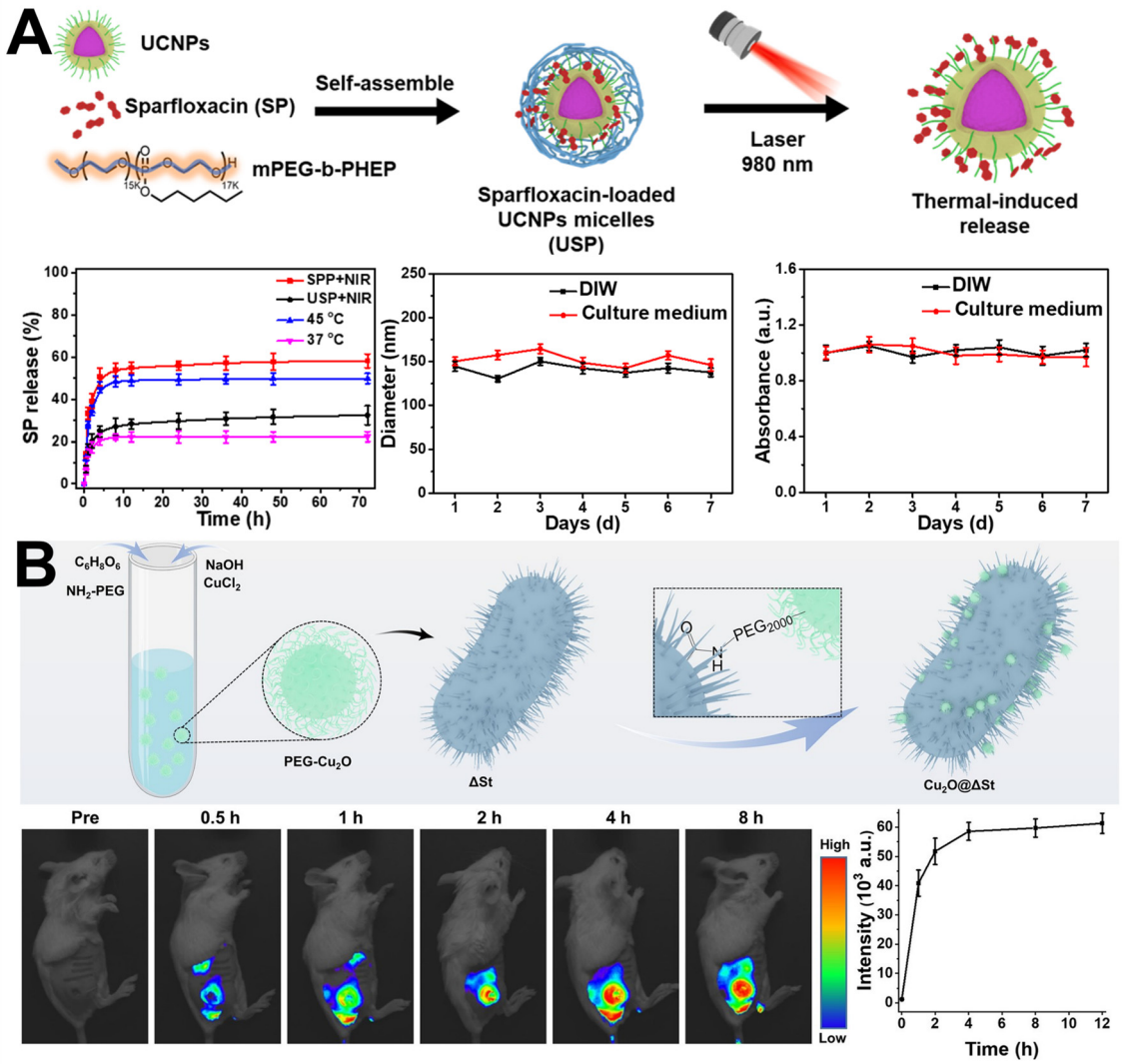

Fig. 11 Specific killing of tumour cells based on biomaterial surface modifications: (A) PPIR780-ZMS enhances CDT by photothermal release of biomaterials. Reproduced with permission from ref. 123. Copyright 2022, American Chemical Society. (B) Cu_2O@ΔSt utilizes anaerobic bacteria to target tumour sites to consume H_2S to enhance PTT and CDT. Reproduced with permission from ref. 124. Copyright 2022, Springer Link.

from the acidic TME promoted the Fenton reaction and produced $^{\bullet}OH$ to enhance CDT. Using the anaerobic properties of different bacteria to target the tumour site, synergistic PTT and CDT can kill tumour cells safely. The cell membranes in organisms also exhibit good biosafety. For example, Jiang *et al.* used iRGD peptide-modified erythrocyte membranes to camouflage GDYO@PEG nanosheets to prolong blood circulation time and enhance extravascular and hypoxic penetration through functional iRGD peptides.[153] iRGD peptide-modified GDYO nanosheets thermally released O_2 and $^1O_2$ to relieve hypoxia at the tumour site and enhanced PTT and CDT to kill tumour cells selectively after light exposure.

However, specific treatments with erythrocyte membrane-modified materials lack targeting abilities. Tumor cell membrane-modified nanosystems have been used to improve nanomedicine targeting function and chemotherapeutic efficacy.[4,154–156] Zhang *et al.* utilized homologous cell membrane-modified platinum-doped hollow dopamine NPs combined with Ce6 (C) and chloroquine (C) to enhance the effect of sonodynamic therapy (SDT) (Fig. 12A).[125] When tumour cells internalized chemoacidic cleavage of the cell membrane, leading to material release, HP and Pt enhanced the Fenton reaction based on their enzyme-like activities and synergistically blocked autophagic fluxes with Ce6 and CQ in the presence of US. This enhanced the effect of SDT, induced apoptosis and iron detachment, and ultimately achieved differential killing of tumour cells.

3.4.2. Surface charge. The surface charge properties of NPs greatly influence their pharmacokinetics and blood circulation, RES clearance, and cellular uptake.[157,158] NPs bearing positive surface charges are more likely to be internalised into negatively charged tumour cells through electrostatic attraction-mediated interactions.[159,160] Positively charged polymer–drug couplings promote tumour infiltration by triggering

endothelial cell cytosis, which leads to rapid extravasation and efficient cancer cell cytosis, greatly enhancing the coupling infiltration into the tumour.[161] For example, Ma *et al.* developed multilayered reactive micelles as multifunctional polymer–drug couplings *via* RAFT reactions to maximise penetration and therapeutic efficacy against Michigan Cancer Foundation-7 tumours by combining positively charged surfaces and size contraction.[126] Xie *et al.* utilized the same strategy by coating bioactive nanovaccines with a PEG shell that could be shed in response to a weakly acidic TME; the size reduction and positive charge increase may have led to deeper drug penetration into the tumour.[162] Bioactive nanovaccines were demonstrated to significantly enhance antigen presentation and drug translocation from DCs into M1-like TAMs and tumour cells by decreasing the size and increasing the positive charge induced by weakly acidic TME.

However, positively charged surfaces in blood circulation readily bind to negatively charged proteins, which can then be removed.[163] Therefore, ideal NPs should maintain a negative charge while in circulation and rapidly change to a positive charge at the tumour site. Li *et al.* presented a novel approach involving the design of adaptive nanogels made of chitosan-polypyrrole (CH-PPy) for improved therapeutic agent delivery in tumour treatment (Fig. 12B).[127] This study aimed to enhance chemotherapy efficacy by using ultrafast charge-reversible CH-PPy-OH-4 NGs (R-NGs), where the CH-PPy polymer is cross-linked with glutaraldehyde and subsequently treated with an alkaline solution. The R-NGs exhibited a negative charge at physiological pH and switched to a positive charge under slightly acidic conditions. Consequently, they were able to convert their negative charge to positive and enable responsive drug delivery, thereby enhancing chemotherapy effectiveness

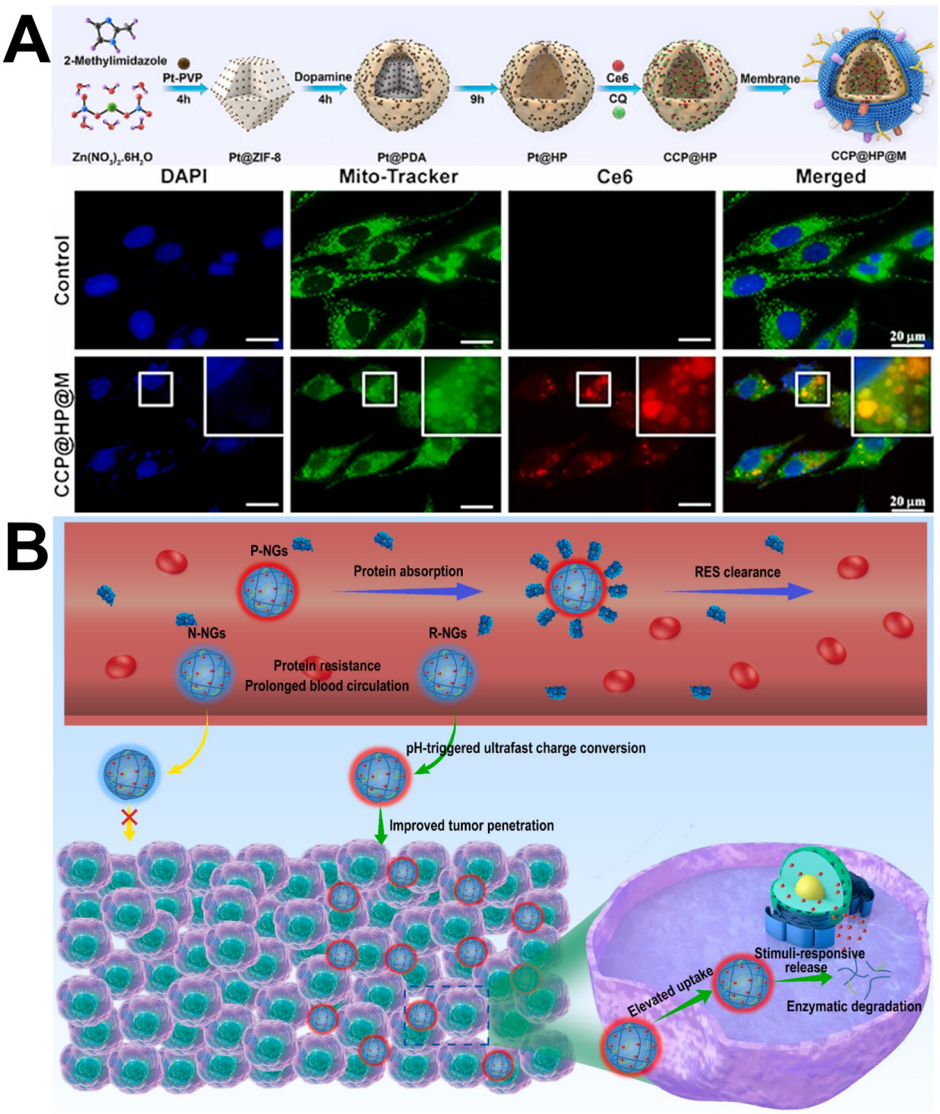

Fig. 12 Specific killing of tumour cells based on biomaterial surface modifications: (A) CCP@HP@M cell membrane modifications target tumour acid release to enhance SDT. Reproduced with permission from ref. 125. Copyright 2023, Elsevier Ltd. (B) pH-responsive charge differences in R-NGs enhance chemotherapy. Reproduced with permission from ref. 127. Copyright 2021, Elsevier Ltd.

for ovarian cancer *in vivo*. Yan *et al.* reported a bone-targeted protein nanomedicine that provided bone targeting by coating the nanomedicine with the anionic polymer poly(aspartic acid) to shield the NP positive charge and shift the surface charge from negative to positive after localisation at the tumour site of the extracellular acidic triggering of tumour cells.[164]

3.5. External energy stimulation

3.5.1. Light. In phototherapy, a diseased area is irradiated with a light source, which kills tumour cells by generating heat and toxic ROS through a phototherapeutic agent (PA) or by releasing a drug. Phototherapy currently consists of three primary forms: PDT, PTT, and light-controlled release of drugs (Fig. 13).[165–167] Phototherapy is noninvasive, localised, and selective. However, its visible-light penetration may be too weak to reach the lesion, and tumour site hypoxia may create a shortage of the oxygen molecules needed to generate ROS.

In PDT, a photosensitive material is exposed to a specific light wavelength, which causes tumour cells at the site to produce ROS, achieving a therapeutic effect.[168] PDT, therefore, requires three factors: a PS, a specific wavelength light source, and an oxygen molecule in the TME.[169] Current widely used PS molecules include protoporphyrin IX (PpIX), methylene blue, and Ce6, as well as the inorganic NPs TiO_2 and ZnO. Although they generate ROS efficiently, these PS substances have excitation wavelengths concentrated in the visible and red light regions (<700 nm).[170] They also have poor water solubility, which reduces their $^1O_2$ yield and consequent PDT efficiency. Liu *et al.* used apoptosis to amplify porphyrin nanofibril assembly, which addressed poor PS water solubility to enhance PDT in oral squamous cell carcinoma.[128] Upon cysteine asparaginase-3 cleavage and laser irradiation, the water-soluble porphyrin derivative Ac-DEVDD-TPP was converted to D-TPP and self-assembled into porphyrin nanofibres, which induced effective apoptosis and pyroptosis for an enhanced PDT effect (Fig. 14A).

Fig. 13 Schematic diagram of a biomaterials system designed based on light response for specific cytotoxicity.

PDT also requires a light source with a specific wavelength; 660, 808, 980, and 1064 nm are commonly used. The third requirement is oxygen molecules. The photosensitive substance transfers light energy to the oxygen molecule, generating ROS, including cytotoxic free radicals and $^1O_2$ species. To eradicate tumours, PS is often used repeatedly to maximise its effectiveness. Therefore, Yang *et al.* developed acid-activated graphene quantum dot nanotransformers (GQD NTs) as photosensitiser carriers capable of both long-term tumour imaging and repetitive PDT.[129] In this study, GQD NTs guided by the Arg-Gly-Asp peptide enabled active tumour site targeting, tumour acid relaxation and amplification, and prolonged tumour retention, thus solving the problems of targeting and low drug utilisation. However, PDT also has drawbacks: it is expensive and cannot be mass-produced. The agents have poor penetration and cannot reach deep lesions. PS molecules can remain in the skin and cause light sensitivity; therefore, bright light must be avoided for three to four weeks after treatment.

The second type of phototherapy, PTT, refers to the use of a specific wavelength light source to irradiate a photothermal agent, which heats the agent and thus kills the tumour cells.[171] Our group obtained hollow $AgBiS_2$ nanospheres with a narrow band gap by rapid precipitation in a weakly polar solvent; these nanospheres exhibited enhanced light absorption and high photothermal conversion efficiency (44.2%) (Fig. 14B).[130] In addition, the hollow-structured $AgBiS_2$ nanospheres were found to possess peroxidase-mimetic features, which combined with the photothermal effect to induce cancer cell-specific cytotoxicity while exhibiting negligible cytotoxicity to normal cells. This effect was attributed to the nanosphere-catalyzed, efficient production of highly reactive •OH from overexpressed H_2O_2 in the TME.

Some studies have combined existing PDT and PTT to achieve synergistic effects. The combined benefits of this synergistic strategy are expected to overcome PTT heat shock effects and TME hypoxia, ultimately improving the effectiveness of tumour phototherapy. Recently, Tang *et al.* designed tumour cell membrane-targeted aggregation-induced emission of photosensitive dimers for synergistic tumour immunotherapy mediated by photodynamic and photothermal effects.[131] The photosensitive dimers effectively generated type I ROS in hypoxic tumour tissues by PDT, which led to focal death through direct cell membrane damage and was further intensified by the dimer photothermal effects. In addition, the enhanced immunogenic cell death (ICD) effect, based on dimerisation, enhanced systemic antitumour immunity to overcome apoptosis resistance and immunosuppression of tumour cells.

At present, most clinical tumour treatments are still based on traditional drug release and chemotherapy, which suffer from low drug release efficiency, poor targeting, and low drug utilisation. Light makes light-controlled drug release a

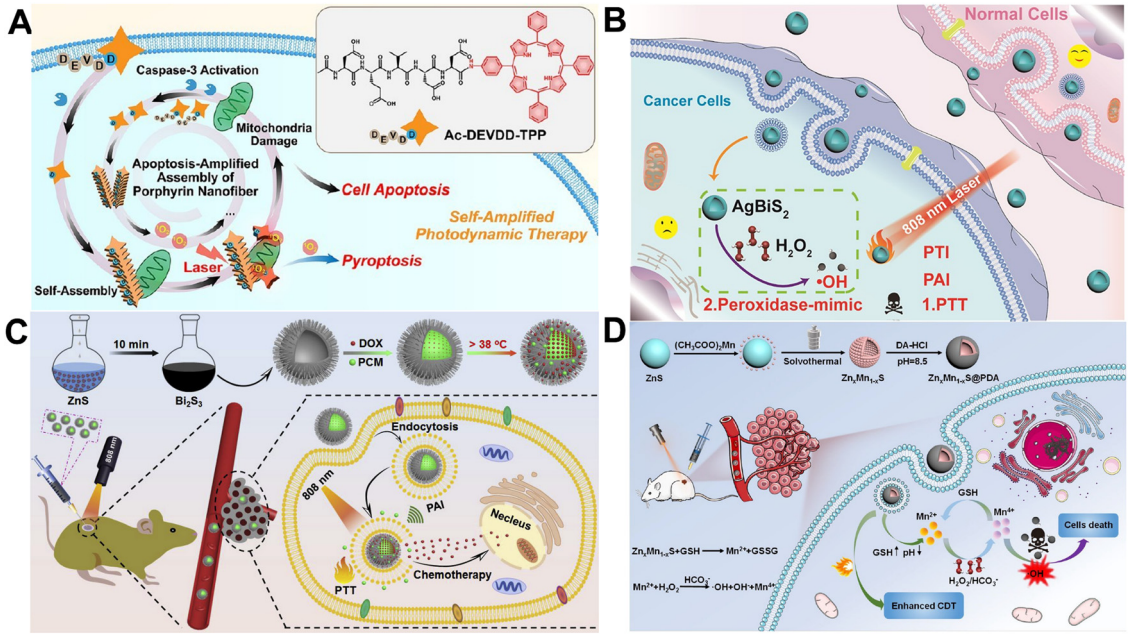

Fig. 14 Phototherapy-based specific killing of tumour cells: (A) Ac-DEVDD-TPP amplifies apoptosis to enhance PDT. Reproduced with permission from ref. 128. Copyright 2023, American Chemical Society. (B) $AgBiS_2$ narrow bandgap enhances PTT. Reproduced with permission from ref. 130. Copyright 2020, American Chemical Society. (C) U-BSHM photothermally phases PCM to release DOX to enhance chemotherapy. Reproduced with permission from ref. 132. Copyright 2020, Elsevier Ltd. (D) $Zn_xMn_{1-x}S$@PDA enhances CDT by photothermal release of biomaterials. Reproduced with permission from ref. 133. Copyright 2021, American Chemical Society.

promising delivery method because of its safe, noninvasive, and spatiotemporally controllable characteristics. Drug release at the lesion site is precisely tuned by adjusting the light source wavelength and intensity, as well as exposure time and space, so that the drug delivery system undergoes heterogeneous morphological changes or degradation.[172] We synthesised hollow Bi_2S_3 microspheres with rod-based urchin-like nanostructures, which could be used as carriers for photocontrolled drug release, using the hard template method *via* a simple, rapid ion exchange (Fig. 14C).[132] A mixture of tetradecanol (phase change material) and DOX was loaded into the hollow cavity and irradiated by an 808 nm laser to heat Bi_2S_3. The excellent thermal effect caused structural changes in the phase change material, triggering DOX release from the hollow interior to achieve a targeted, quantitatively controllable light release. Therefore, such sea urchin-like hollow nanostructures are important candidates for photocontrollable drug release in tumours. In addition to photocontrolled drug release, our group also constructed $Zn_xMn_{1-x}S$ epitaxially grown PDA NPs (ZMS@PDA) for photothermally controlled metal ion release (Fig. 14D) based on the excellent photothermal conversion efficiency of PDA.[133] Under 808 nm laser irradiation, heat promoted Mn^{2+} release and enhanced the Mn^{2+}-driven Fenton-like reaction to generate a large amount of ROS, killing the tumour cells. In addition, ZMS@PDA exhibited good biocompatibility with normal cells.

In many experimental cases, the desired results could not be achieved using only one type of light therapy. Zhang *et al.* combined three phototherapeutic modalities to achieve a synergistic effect on tumour treatment.[134] They developed a platelet smart-navigation carrier for photothermal cancer chemotherapy and used it for the controlled, visible release of therapeutic tumour drugs. A platelet-based carrier loaded with DOX and the photothermal agent IR-820 provided PTT-based imaging navigation for platelet carriers with a drive and loading system. The smart platelet carrier achieved deep penetration for tumour targeting, fluorescence imaging guidance, light-controlled drug release, and chemo–PTT combination, providing a new approach for the precise drug delivery and efficient treatment of tumours.

Radiotherapy (RT), which is also essentially a form of phototherapy, is one of the key methods of cancer treatment and is used to control and reduce tumour growth by destroying the deoxyribonucleic acid (DNA) of cancer cells through high-energy radiation.[173,174] However, some cancers show RT resistance, and the side effects affect the patient quality of life. In recent years, RT sensitisation technology has provided a new way to solve these problems.[175] In RT sensitisation, other drugs or treatments are used concurrently with RT to increase the tumour radiation sensitivity, enhancing the therapeutic effect.[176] With RT sensitisation, the radiation dose can be reduced, side effects can be mitigated, and treatment effectiveness can be improved. Strategies for RT sensitisation include concurrent use of chemotherapy, immunotherapy, and oxidative stress.[177] However, TME hypoxia and GSH overexpression, which maintain an immunosuppressive microenvironment and promote DNA repair, greatly limit the efficacy of RT sensitisation.[178] To address these issues, our group developed

4T1 cell membrane-encapsulated $Bi_{2-x}Mn_xO_3$ nanospheres (T@BM), a regimen that demonstrated enhanced therapeutic efficacy with a combination of RT and immunotherapy.[179] The cancer cell membrane-encapsulated T@BM prolonged the blood circulation time. The T@BM produced O_2 *in situ* and consumed GSH to amplify DNA damage and remodel the tumour's immunosuppressive microenvironment, enhancing the RT efficacy. Meanwhile, the released Mn^{2+} can activate STING pathway-induced immunotherapy, increasing the immune infiltration of *in situ* breast tumours. Thus, RT sensitisation has great potential for clinical applications. It can improve treatment efficacy, reduce side effects, shorten treatment time, and help treat refractory tumours. However, RT sensitisation faces challenges such as drug selection, dose determination, and treatment sequence, which must be addressed in further research and clinical trials.

3.5.2. Sound. SDT is a new approach to tumour treatment.[180] The advantages of SDT include its noninvasiveness, targeting accuracy, safety, and reproducibility. SDT is based on using a high concentration of acoustic sensitisers (ASs) to target and aggregate tumour and neovascular endothelial cells. After imaging and precise localisation under noninvasive conditions, ultrasound of a specific wavelength activates the AS, causing it to react to produce $^1O_2$ chemically. Electrons are then removed from the tumour cells, and most of the tumour cell organelles are destroyed by TEM, leading to cell death. Metal NPs are often used as ultrasonic sensitisers. For example, Zhang *et al.* developed and utilised a metal nanoparticle chalcogenide-based $ZnSnO_3$:Nd phase engineering strategy to improve the efficiency of the acoustic tumour dynamic treatment (Fig. 15A).[135] In the engineered crystalline chalcogenide $ZnSnO_3$:Nd, Nd^{3+} replaced Zn^{2+} to move the nonbonded state of O 2p toward the Fermi energy level. The ultrasonic sensor energy band structure was optimised by reducing its bandgap. Inhomogeneous charge substitution can also form electron traps and oxygen vacancies, shorten the electron migration distance, accelerate electron–hole separation, and inhibit carrier complexation, thus improving acoustic sensitivity.

In addition to SDT, ultrasound has enabled precise control of drug carriers in time and space and precise control of tissue penetration depth and energy. For example, Huo *et al.* used ultrasound to break mechanochemically unstable covalent and weak noncovalent bonds to activate drugs in inactive macromolecules or nanocomponents.[136] They discovered that polymers with disulphide sequences at the central position of the backbone can release alkaloidal anticancer drugs from β-carbonate linkers *via* force-induced intramolecular 5-exo-delta cyclisation. Secondly, aminoglycoside antibiotics act synergistically with the polyadaptor ribonucleic acid structure and are activated by mechanochemical actions that open and break the nucleic acid backbone. Finally, nanoparticle–polymer and nanoparticle–nanoparticle combinations of the peptide antibiotic vancomycin bound to its complementary peptide target *via* hydrogen bonding were activated by force-induced hydrogen bond breaking. This work reported by the authors of this paper demonstrates the potential of ultrasonic activation of mechanically active prodrug systems.

3.5.3. Magnetism. Magnetothermal therapy (MTT) has become a clinical treatment for malignant tumours. Its principle of action is through the thermal induction of magnetite NPs (MNPs) under an external alternating magnetic field (AMF).[125–137,140,141,153–181] MTT has significant advantages over PDT and PTT because of its ability to reach deeper tissue levels and target and kill tumour cells without damaging the surrounding healthy tissue. Such targeting properties can be further enhanced by artificially coupling specific ligand receptors to MNPs.[182] Typically, MTT tumour therapy relies on external heating of tumour cells; a temperature at the observable lesion site higher than 43 °C is considered a key predictor of MTT tumour inhibition and therapeutic efficacy. However, MTT alone is too inefficient. To overcome this shortcoming, Liu *et al.* mediated magnetothermodynamic therapy through graphene oxide-grafted magnetic nanorings (VIOs-GO), thereby achieving results that favoured ROS-related immune responses and synergistically enhanced tumour therapy (Fig. 15B).[137] The VIOs-GO nanoplatforms have a high thermal conversion efficiency and can significantly increase ROS levels under AMF. This is supported by the exposure of 4T1 breast cancer cells to calreticulin, which directly promotes macrophage polarisation to a pro-inflammatory M1 phenotype and further elevation of tumour-infiltrating T lymphocytes.[183] The authors and others overcame the poor thermal conversion efficiency of MNPs. By exploiting ROS-mediated immune effects, the antitumour capabilities of future cancer magnetotherapy could significantly improve.

3.5.4. Electricity. Electrodynamic therapy (EDT) utilises an electrically driven, catalytic reaction of platinum NPs in an electric field to induce ROS production for cancer treatment by triggering water molecule decomposition.[139,184] EDT offers several advantages over current ROS-based therapies, such as electric remote control feasibility and few side effects. Chen *et al.* developed DOX-loaded porous platinum NPs (pPt NPs) for EDT (Fig. 15C).[140] These pPt-PEG NPs generate ROS by triggering water decomposition under an electric field; ROS can induce the inhibition of P-glycoprotein, which in turn enhances the chemotherapeutic agent efficacy by promoting intracellular accumulation of the drug. EDT is a new type of tumour therapy that combines chemotherapeutic drugs with pulsed electrical currents to achieve targeted killing of tumour cells without damaging the surrounding healthy cells and tissues.[185] Experiments suggest that electrical stimulation of tumour cells weakens the cell outer membranes, allowing chemotherapeutic drugs that work synergistically to function more effectively, better access the lesion site, and ultimately kill the tumour cells.

3.5.5. Force. Microneedles (MNs) are a novel physical transdermal drug delivery tool consisting of multiple micron-sized (or even smaller) tiny tips attached to a base in an array, with the body of the needle typically 10–2000 microns high and 10–50 microns wide.[186–188] MNs can pass directionally through the stratum corneum, creating micrometer-scale mechanical

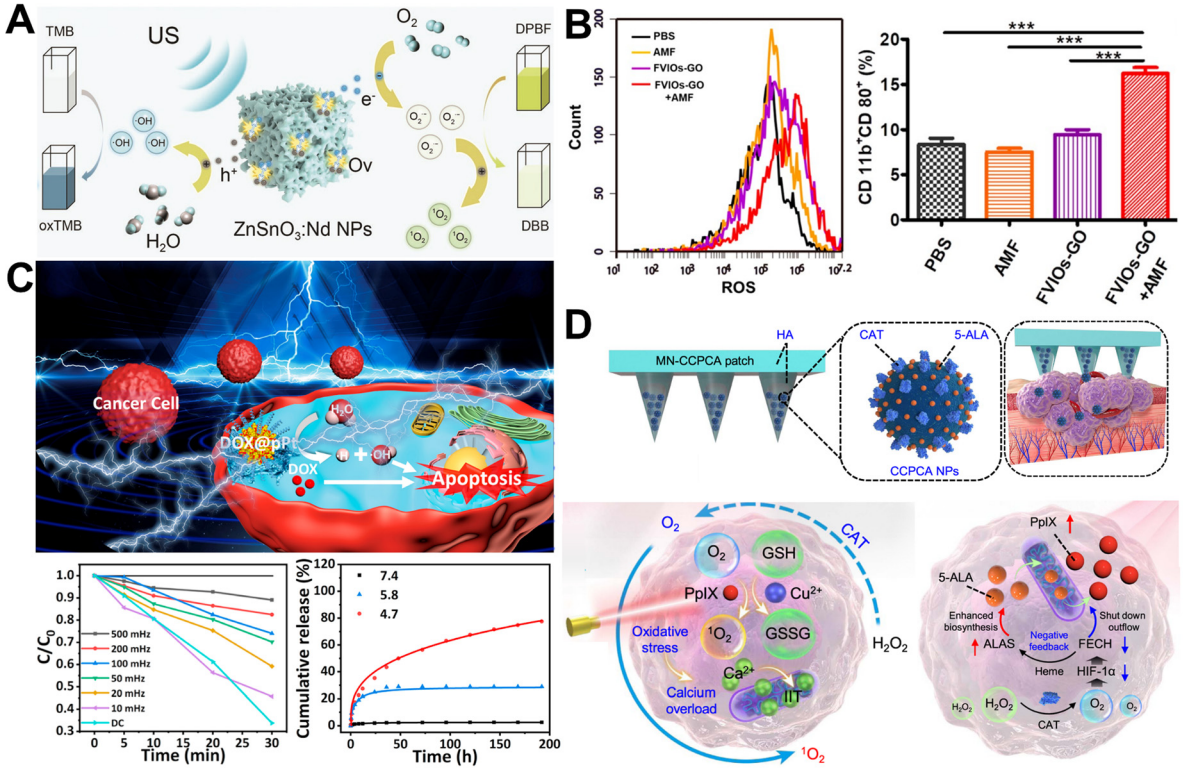

Fig. 15 Biomaterials based on acoustic, magnetic, electrical, and force stimulation for specific tumour cell killing: (A) $ZnSnO_3$:Nd NPs used to augment SDT for tumour treatment. Reproduced with permission from ref. 135. Copyright 2023, Wiley-VCH. (B) FVIOs-GO-CREKA NPs are effective in the treatment of breast cancer *via* MTD. Reproduced with permission from ref. 137. Copyright 2020, American Chemical Society. (C) DOX@pPt kills tumours by electrically stimulating water decomposition to produce •OH. Reproduced with permission from ref. 140. Copyright 2020, Elsevier Ltd. (D) MN-CCPCA microneedle patches are used for imageable tracking and PDT for tumour treatment. Reproduced with permission from ref. 141. Copyright 2022, Nature Publishing Group.

channels that can place drugs directly on the epidermis or upper dermis. They can participate in microcirculation and produce pharmacological responses even without passing through the stratum corneum.[189] MNs can pass through the dermal skin surface but do not reach the subcutaneous tissue or contact its peripheral nerves, so there is no pain, trauma, or other side effects.[190] Traditional MNs include silicone (which is not biocompatible and breaks easily with processing), metal, glass, and polymer MNs (which are biocompatible and biodegradable).[191]

Differences in MN materials and composition can lead to differences in drug delivery efficiency and administration mode. The MNs currently available face the following problems: (1) the microneedles must have sufficient strength and stiffness to penetrate the skin; (2) the microneedle force on the skin must be small enough to be painless and minimally invasive; and (3) the microneedles need good biocompatibility. To solve these problems and exploit the advantages of MNs in tumour treatment, He *et al.* implemented and used highly biocompatible transdermal microneedle patches that can be used for imageable tracking and PDT for tumour treatment based on traditional therapeutic modalities (Fig. 15D).[141] The patch integrated 5-aminolevulinic acid- and CAT-coloaded, tumour acid-responsive, copper-doped calcium phosphate NPs, which greatly enhanced the photodynamic therapeutic efficacy of 5-aminolevulinic acid by maximising PpIX aggregation in the tumour. Peroxidase maintained oxygen production *in vivo* and upregulated protoporphyrin IX (PpIX) biosynthesis by blocking PpIX efflux, thereby enhancing its accumulation. This approach helps to optimise the therapeutic parameters for different cancers and enables reproducible PDT enhanced by Ca^{2+}/Cu^{2+} interference, making this therapeutic patch promising for clinical applications.

4. Conclusions and perspectives

In this review, we firstly introduced the differences between tumour and normal cells and tissues, including the differences in glucose, lactate, acidity, redox balance, and surface receptors at the cellular level, and the ECM, tumour vasculature system, SCs, immune cells, and others at the tissue level. The research progress in this field was summarised and discussed.[192–195] Current strategies for nanosystem construction were described in detail, including the varying of composition, particle size, shape, structure, surface functionalisation, and external stimulation capability. Careful design and construction of nanosystems can achieve personalised, targeted tumour therapy to

meet the needs of differential treatment.[196–198] This innovative therapeutic approach is expected to improve therapeutic efficacy, reduce adverse effects, and improve survival and quality of life in patients with tumours. However, challenges remain, some of which are technical, whereas others may be related to clinical applications and therapeutic efficacy (Fig. 16).

There are still some concerns regarding the toxic effects of foreign substances on organisms. Heterogeneity between different tumours and within the same tumour may affect a nanosystem delivery and targeting effectiveness, because different cells may have different nanosystem uptake and responses. Therefore, different nanosystems should be designed and prepared for different tumour types. Current research is directed toward specific treatments for different tumour types, but additional work is needed.[199] For example, mouse tumour models are usually subcutaneous tumours, which may be due to the difficulty of the modelling technique or time constraints. When conducting animal experiments, *in situ* tumour or transplanted tumour models should be recommended. Collaboration with relevant hospitals and tumour patients should be required to create *in vivo* mouse models closer to human tumours for clinical translation.

In the realm of nanomedicine synthesis design, our innovative approach focuses on creating sophisticated nanomedicines that are specifically crafted to maintain inertness under typical physiological conditions. This deliberate design ensures that these nanomedicines remain stable and inactive, avoiding any unintended interactions or side effects within the body's normal environment. However, they are ingeniously engineered to activate upon exposure to specific external physical stimuli, such as magnetic fields, light, or heat. Upon encountering these targeted stimuli, these nanomedicines undergo a precise transformation into active therapeutic agents, thereby delivering their intended effects exactly when and where they are needed, optimizing therapeutic outcomes while minimizing potential side effects. However, the following issues need to be addressed for practical applications as follows.

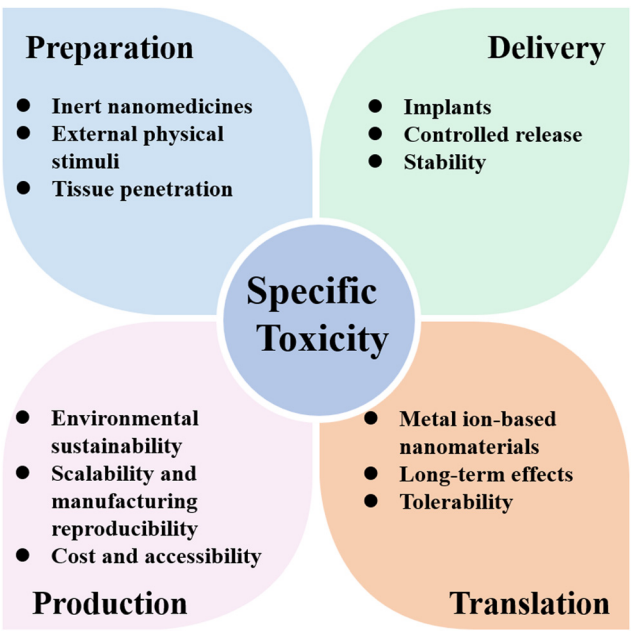

Fig. 16 Challenges and perspectives of tumour killing based on specific toxicity.

The first one is the tissue penetration: visible and UV light, which have limited penetration depth in biological tissues, have difficulty reaching deep tumours.[200] NIR light, ultrasound, and magnetism can penetrate more deeply into tissues and improve the efficacy of deep tumour treatments. Therefore, different tumour models require the selection of appropriate stimulation sources and investigation of multiple stimulus-response systems to improve overall medication efficacy and reduce reliance on any single modality. Side effects: side effects such as phototoxicity, ultrasound cavitation, overheating caused by photothermal magnetic heating, and potential tissue loss from microneedling affect stimulation usability.[201] Combining nanomedicine enrichment, such as localised activation through ligand–receptor interactions, can potentially reduce side effects. Advanced imaging techniques (such as MRI, PET, and CT) have been employed to guide and monitor the delivery and effects of stimulus-responsive therapies. Integrated systems now exist that allow real-time monitoring and adjustment of therapies to ensure the precise control of therapeutic parameters.

The second one is the delivery technology, employing implants emerges as a promising and innovative strategy to significantly enhance therapeutic outcomes and effectively mitigate concerns related to drug toxicity. This method involves the strategic placement of biocompatible implants within the body, which can provide a controlled and sustained release of therapeutic agents over extended periods. The use of implants offers the potential to precisely deliver therapeutic agents to targeted sites, ensuring that the medication reaches the specific area where it is needed most. This targeted delivery not only optimizes the efficacy of the treatment by maintaining appropriate drug levels at the site of action but also minimizes systemic side effects by reducing the overall exposure of the body to the drug. Consequently, this approach can improve patient compliance, reduce the frequency of dosing, and enhance the overall therapeutic experience. Nanomedicine delivery must also overcome challenges—controlled release: ensuring that the drug is released at the appropriate time and rate, which is crucial to maximise therapeutic efficacy while minimising side effects. Nanoparticles that respond to specific physiological triggers (such as pH, temperature, enzymes, and immune activation) represent progress toward this goal.[33] Precise control of where the drug is released in the body or within specific tissues can improve therapeutic efficacy. Stability: ensuring nanoparticle stability during storage and drug delivery is critical, including the prevention of premature degradation or aggregation, which can affect drug performance. Formulations are required to enhance nanomedicine stability and bioavailability while maintaining their therapeutic properties over time.

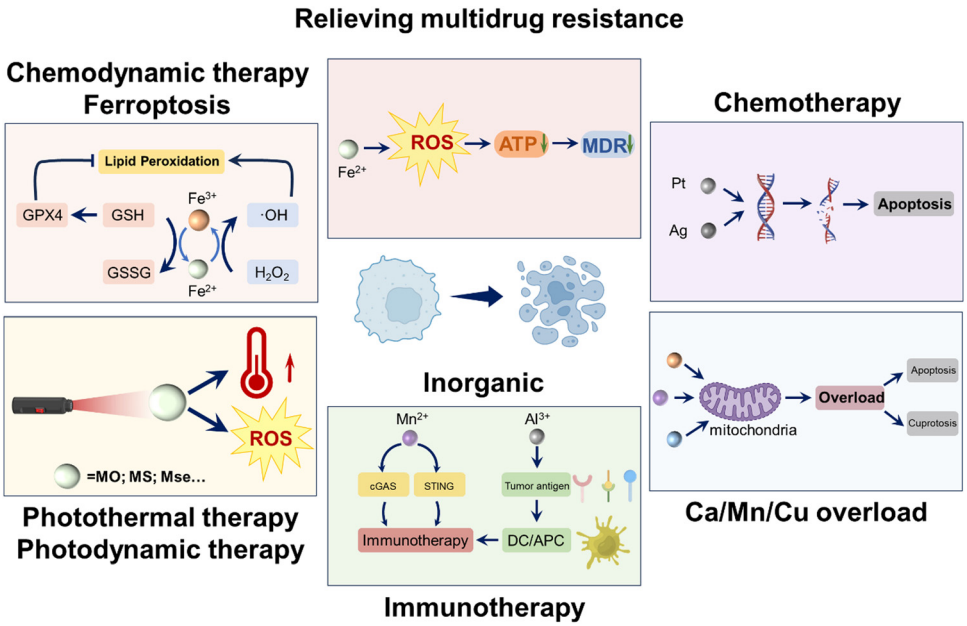

Fig. 17 Different roles of metal ions.

Among them, the production is crucial to tailor synthetic methods and techniques to facilitate scalability and seamless integration into industrial processes. These advancements should prioritize environmental sustainability and economic feasibility, aiming to enhance efficiency while reducing ecological impact. Nanomedicine synthesis for future clinical applications possesses several key features––scalability and manufacturing reproducibility: achieving consistency in nanomedicine quality and performance for large-scale production will be challenging. Small variations in particle size, shape, and surface features can significantly affect their efficacy and safety. Nanomedicine synthesis generally involves multiple steps, including precisely controlled nanomaterial assembly, functionalisation, and loading with therapeutic agents. These complex processes will be challenging to scale up while maintaining quality assurance. Therefore, standardised protocols for nanomedicine synthesis and characterisation are necessary to ensure reproducibility and quality control across different batches. The use of advanced manufacturing techniques, such as microfluidics and continuous-flow reactors, can improve nanomedicine production scalability and consistency. The use of automated systems for synthesis and real-time quality control can reduce batch variation and improve reproducibility. Cost and accessibility: the complex, sophisticated processes involved in synthesizing nanomedicines often lead to high production costs, rendering their widespread clinical use more difficult.[202] Balancing development and manufacturing costs with healthcare system pricing and reimbursement is critical to nanomedicine economic viability. Cost-effective synthesis methods and optimized production processes can help reduce the overall cost of nanomedicine manufacturing and are urgently needed. Economies of scale through mass production and widespread adoption can reduce nanomedicine unit costs.

Clinical studies should focus on the long-term effects and tolerability of these nanosystems. The safety of nanosystems must be fully validated before their clinical application.[203,204] Therefore, in nanosystem construction, biomaterials or drugs that have been clinically applied or approved by the Food and Drug Administration should be utilised whenever possible to avoid biomaterial toxicity. Metal ion-based nanomaterials can form drug-free therapeutic nanoplatforms, in which the metal ions are used as building nanomaterials instead of conventional drugs (Fig. 17). The effects of different nanosystem components on other body systems, which may have promoting or damaging impacts on other tissues, should be monitored for a long time. The mechanism and specific amount of action should be clarified.[205,206] For example, the short-term toxicity of metal ions in inorganic nanosystems has been extensively studied, but their effects on *in vivo* models several months after treatment are less well documented. Short-term therapeutic effects may differ from long-term effects, therapeutic and other, and tolerability issues may limit treatment sustainability.[207] In addition, the introduction of nanosystems into clinical applications must meet stringent regulatory and supervisory requirements. In summary, translating nanosystems from laboratory to clinical applications involve numerous challenges, including safety, efficacy, manufacturing, individual differences, and regulation. Interdisciplinary research and clinical trials will be key to addressing these challenges for the successful application of nanosystems in oncology.[208]

In conclusion, specific toxicity therapies offer unprecedented opportunities for tumour therapy. Nanosystem-based toxicity therapy has multiple advantages over traditional therapeutic approaches, such as enhanced targeting, reduced toxicity, fewer side effects, the ability to overcome drug resistance, and improved drug stability. These advantages can greatly

improve tumour therapy effectiveness, reduce patient suffering, and provide an important means for individualised precise treatment.

Author contributions

Zhaoyou Chu, Wanni Wang, and Wang Zheng wrote and revised the paper. Wanyue Fu and Yujie Wang helped paper revision and drew the figures in the paper. Hua Wang and Haisheng Qian put forward the idea and supervised the review writing and revision.

Data availability

No primary research results, software or code have been included and no new data were generated or analysed as part of this review.

Conflicts of interest

There are no conflicts to declare.

Acknowledgements

This work was financially supported by the National Natural Science Foundation of China (Grants 52172276).

References

1 E. O. Aboagye, T. D. Barwick and U. Haberkorn, *Ca-Cancer J. Clin.*, 2023, **73**, 255–274.
2 M. D. Ilie, A. Vasiljevic, P. Bertolino and G. Raverot, *Endoc. Rev.*, 2022, **44**, 297–311.
3 J. G. Nicholson and H. A. Fine, *Cancer Discovery*, 2021, **11**, 575–590.
4 R. H. Fang, W. Gao and L. Zhang, *Nat. Rev. Clin. Oncol.*, 2023, **20**, 33–48.
5 M. P. Vincent, J. O. Navidzadeh, S. Bobbala and E. A. Scott, *Cancer Cell*, 2022, **40**, 255–276.
6 A. L. Facklam, L. R. Volpatti and D. G. Anderson, *Adv. Mater.*, 2020, **32**, 1902005.
7 X. Kong, R. Cheng, J. Wang, Y. Fang and K. C. Hwang, *Nano Today*, 2021, **36**, 101004.
8 D. Peer, J. M. Karp, S. Hong, O. C. Farokhzad, R. Margalit and R. Langer, *Nat. Nanotechnol.*, 2007, **2**, 751–760.
9 J. Bariwal, H. Ma, G. A. Altenberg and H. Liang, *Chem. Soc. Rev.*, 2022, **51**, 1702–1728.
10 M. Chehelgerdi, M. Chehelgerdi, O. Q. B. Allela, R. D. C. Pecho, N. Jayasankar, D. P. Rao, T. Thamaraikani, M. Vasanthan, P. Viktor, N. Lakshmaiya, M. J. Saadh, A. Amajd, M. A. Abo-Zaid, R. Y. Castillo-Acobo, A. H. Ismail, A. H. Amin and R. Akhavan-Sigari, *Mol. Cancer*, 2023, **22**, 169.
11 D. Fan, Y. Cao, M. Cao, Y. Wang, Y. Cao and T. Gong, *Signal Transduct. Target. Ther.*, 2023, **8**, 293.
12 J. Chen, Y. Zhu, C. Wu and J. Shi, *Chem. Soc. Rev.*, 2023, **52**, 973–1000.
13 Q. Peña, A. Wang, O. Zaremba, Y. Shi, H. W. Scheeren, J. M. Metselaar, F. Kiessling, R. M. Pallares, S. Wuttke and T. Lammers, *Chem. Soc. Rev.*, 2022, **51**, 2544–2582.
14 N. Singh, S. Son, J. An, I. Kim, M. Choi, N. Kong, W. Tao and J. S. Kim, *Chem. Soc. Rev.*, 2021, **50**, 12883–12896.
15 I. Martinez-Reyes and N. S. Chandel, *Nat. Rev. Cancer*, 2021, **21**, 669–680.
16 M. Binnewies, E. W. Roberts, K. Kersten, V. Chan, D. F. Fearon, M. Merad, L. M. Coussens, D. I. Gabrilovich, S. Ostrand-Rosenberg, C. C. Hedrick, R. H. Vonderheide, M. J. Pittet, R. K. Jain, W. Zou, T. K. Howcroft, E. C. Woodhouse, R. A. Weinberg and M. F. Krummel, *Nat. Med.*, 2018, **24**, 541–550.
17 Z. Tang, P. Zhao, H. Wang, Y. Liu and W. Bu, *Chem. Rev.*, 2021, **121**, 1981–2019.
18 Q. Q. Tang, R. Q. Wu, H. M. Fan, X. L. Liu and Y. Lu, *Prog. Biochem. Biophys.*, 2022, **49**, 2266–2277.
19 H. Amani, M. A. Shahbazi, C. D'Amico, F. Fontana, S. Abbaszadeh and H. A. Santos, *J. Controlled Release*, 2021, **330**, 185–217.
20 S. Liang, X. Deng, P. A. Ma, Z. Cheng and J. Lin, *Adv. Mater.*, 2020, **32**, 2003214.
21 Q. Wu, H. Zhang and H. Liu, *BMEMat.*, 2023, **1**, e12010.
22 Y. Tao, H. F. Chan, B. Shi, M. Li and K. W. Leong, *Adv. Funct. Mater.*, 2020, **30**, 2005029.
23 M. G. Vander Heiden, L. C. Cantley and C. B. Thompson, *Science*, 2009, **324**, 1029–1033.
24 M. Cao, R. Isaac, W. Yan, X. Ruan, L. Jiang, Y. Wan, J. Wang, E. Wang, C. Caron, S. Neben, D. Drygin, D. P. Pizzo, X. Wu, X. Liu, A. R. Chin, M. Y. Fong, Z. Gao, K. Guo, O. Fadare, R. B. Schwab, Y. Yuan, S. E. Yost, J. Mortimer, W. Zhong, W. Ying, J. D. Bui, D. D. Sears, J. M. Olefsky and S. E. Wang, *Nat. Cell Biol.*, 2022, **24**, 954–967.
25 Z. Chu, J. Yang, W. Zheng, J. Sun, W. Wang and H. Qian, *Coord. Chem. Rev.*, 2023, **481**, 215049.
26 G. M. DeNicola, F. A. Karreth, T. J. Humpton, A. Gopinathan, C. Wei, K. Frese, D. Mangal, K. H. Yu, C. J. Yeo, E. S. Calhoun, F. Scrimieri, J. M. Winter, R. H. Hruban, C. Iacobuzio-Donahue, S. E. Kern, I. A. Blair and D. A. Tuveson, *Nature*, 2011, **475**, 106–109.
27 D. Samanta and S. C. Almo, *Cell. Mol. Life Sci.*, 2015, **72**, 645–658.
28 S. Jalkanen, M. Karikoski, N. Mercier, K. Koskinen, T. Henttinen, K. Elima, K. Salmivirta and M. Salmi, *Blood*, 2007, **110**, 1864–1870.
29 S. D. Patel, C. P. Chen, F. Bahna, B. Honig and L. Shapiro, *Curr. Opin. Struct. Biol.*, 2003, **13**, 690–698.
30 J. Kappelmayer and B. Nagy Jr., *Biomed. Res. Int.*, 2017, 6138145.
31 C. Wai Wong, D. E. Dye and D. R. Coombe, *Int. J. Cell Bio.*, 2012, 340296.
32 A. Pérez-González, K. Bévant and C. Blanpain, *Nat. Cancer*, 2023, **4**, 1063–1082.

33 Q. Zhou, J. Xiang, N. Qiu, Y. Wang, Y. Piao, S. Shao, J. Tang, Z. Zhou and Y. Shen, *Chem. Rev.*, 2023, **123**, 10920–10989.
34 S. T. Barry, D. I. Gabrilovich, O. J. Sansom, A. D. Campbell and J. P. Morton, *Nat. Rev. Cancer*, 2023, **23**, 216–237.
35 J. Y. Park, J. Y. Park, Y. G. Jeong, J. H. Park, Y. H. Park, S. H. Kim and D. Khang, *Adv. Mater.*, 2023, **35**, 2300934.
36 M. Scaranti, E. Cojocaru, S. Banerjee and U. Banerji, *Nat. Rev. Clin. Oncol.*, 2020, **17**, 349–359.
37 F. Kai, A. P. Drain and V. M. Weaver, *Dev. Cell*, 2019, **49**, 332–346.
38 E. Henke, R. Nandigama and S. Ergun, *Front. Mol. Biosci.*, 2020, **6**, 00160.
39 C. J. D. Osterman, D. Ozmadenci, E. G. Kleinschmidt, K. N. Taylor, A. M. Barrie, S. Jiang, L. M. Bean, F. J. Sulzmaier, J. Li, X. L. Chen, G. Fu, M. Ojalill, P. Rappu, J. Heino, A. A. Mark, G. Xu, K. M. Fisch, D. T. Weaver, J. A. Pachter, B. Gyorffy, M. T. McHale, D. C. Connolly, A. Molinolo, D. G. Stupack and D. D. Schlaepfer, *Clin. Cancer Res.*, 2020, **26**, 70.
40 A. Wang-Gillam, *J. Clin. Oncol.*, 2019, **37**, 1041–1043.
41 A. D. Rhim, P. E. Oberstein, D. H. Thomas, E. T. Mirek, C. F. Palermo, S. A. Sastra, E. N. Dekleva, T. Saunders, C. P. Becerra, I. W. Tattersa, C. B. Westphalen, J. Kitajewski, M. G. Fernandez-Barrena, M. E. Fernandez-Zapico, C. Iacobuzio-Donahue, K. P. Olive and B. Z. Stanger, *Cancer Cell*, 2014, **25**, 735–747.
42 M. de Palma, D. Biziato and T. V. Petrova, *Nat. Rev. Cancer*, 2017, **17**, 457–474.
43 L. Schito and S. Rey, *Cancer Lett.*, 2020, **487**, 74–84.
44 M. B. Schaaf, A. D. Garg and P. Agostinis, *Cell Death Dis.*, 2018, **9**, 115.
45 J. D. Martin, G. Seano and R. K. Jain, *Annu. Rev. Physiol.*, 2019, **81**, 505–534.
46 A. G. Sorensen, K. E. Emblem, P. Polaskova, D. Jennings, H. Kim, M. Ancukiewicz, M. Wang, P. Y. Wen, P. Ivy, T. T. Batchelor and R. K. Jain, *Cancer Res.*, 2012, **72**, 402–407.
47 T. T. Batchelor, A. G. Sorensen, E. di Tomaso, W. T. Zhang, D. G. Duda, K. S. Cohen, K. R. Kozak, D. P. Cahill, P. J. Chen, M. Zhu, M. Ancukiewicz, M. M. Mrugala, S. Plotkin, J. Drappatz, D. N. Louis, P. Ivy, D. T. Scadden, T. Benner, J. S. Loeffler, P. Y. Wen and R. K. Jain, *Cancer Cell*, 2007, **11**, 83–95.
48 C. G. Willett, Y. Boucher, E. di Tomaso, D. G. Duda, L. L. Munn, R. T. Tong, D. C. Chung, D. V. Sahani, S. P. Kalva, S. V. Kozin, M. Mino, K. S. Cohen, D. T. Scadden, A. C. Hartford, A. J. Fischman, J. W. Clark, D. P. Ryan, A. X. Zhu, L. S. Blaszkowsky, H. X. Chen, P. C. Shellito, G. Y. Lauwers and R. K. Jain, *Nat. Med.*, 2004, **10**, 145–147.
49 L. E. Huang, *Science*, 2013, **339**, 1285–1286.
50 G. N. Masoud and W. Li, *Acta Pharm. Sin. B*, 2015, **5**, 378–389.
51 A. Giaccia, B. G. Siim and R. S. Johnson, *Nat. Rev. Drug Discovery*, 2003, **2**, 803–811.
52 G. L. Semenza, *Nat. Rev. Cancer*, 2003, **3**, 721–732.
53 J. K. Tee, L. X. Yip, E. S. Tan, S. Santitewagun, A. Prasath, P. C. Ke, H. K. Ho and D. T. Leong, *Chem. Soc. Rev.*, 2019, **48**, 5381–5407.
54 J. Fang, W. Islam and H. Maeda, *Adv. Drug Delivery Rev.*, 2020, **157**, 142–160.
55 M. Izci, C. Maksoudian, B. B. Manshian and S. J. Soenen, *Chem. Rev.*, 2021, **121**, 1746–1803.
56 S. Wilhelm, A. J. Tavares, Q. Dai, S. Ohta, J. Audet, H. F. Dvorak and W. C. W. Chan, *Nat. Rev. Mater.*, 2016, **1**, 16014.
57 S. E. McNeil, *Nat. Rev. Mater.*, 2016, **1**, 16073.
58 S. Wilhelm, A. J. Tavares and W. C. W. Chan, *Nat. Rev. Mater.*, 2016, **1**, 16074.
59 K. Igarashi, H. Cabral, T. Hong, Y. Anraku, F. Mpekris, T. Stylianopoulos, T. Khan, A. Matsumoto, K. Kataoka, Y. Matsumoto and T. Yamasoba, *Small*, 2021, **17**, 2103751.
60 M. A. Miller, R. Chandra, M. F. Cuccarese, C. Pfirschke, C. Engblom, S. Stapleton, U. Adhikary, R. H. Kohler, J. F. Mohan, M. J. Pittet and R. Weissleder, *Sci. Transl. Med.*, 2017, **9**, eaal0225.
61 J. Liu, L. Guo, Z. Mi, Z. Liu, P. Rong and W. Zhou, *J. Controlled Release*, 2022, **348**, 1050–1065.
62 Q. Wang, Q. Liang, J. Dou, H. Zhou, C. Zeng, H. Pan, Y. Shen, Q. Li, Y. Liu, D. T. Leong, W. Jiang and Y. Wang, *Nat. Nanotechnol.*, 2024, **19**, 95–105.
63 M. I. Setyawati, C. Y. Tay, S. L. Chia, S. L. Goh, W. Fang, M. J. Neo, H. C. Chong, S. M. Tan, S. C. J. Loo, K. W. Ng, J. P. Xie, C. N. Ong, N. S. Tan and D. T. Leong, *Nat. Commun.*, 2013, **4**, 1673.
64 H. Tang, Y. Zhang, T. Yang, C. Wang, Y. Zhu, L. Qiu, J. Liu, Y. Song, L. Zhou, J. Zhang, Y. K. Wong, Y. Liu, C. Xu, H. Wang and J. Wang, *Nat. Nanotechnol.*, 2023, **18**, 1067–1077.
65 J. Ren, N. Andrikopoulos, K. Velonia, H. Tang, R. Cai, F. Ding, P. C. Ke and C. Chen, *J. Am. Chem. Soc.*, 2022, **144**, 9184–9205.
66 M. Cao, R. Cai, L. Zhao, M. Guo, L. Wang, Y. Wang, L. Zhang, X. Wang, H. Yao, C. Xie, Y. Cong, Y. Guan, X. Tao, Y. Wang, S. Xu, Y. Liu, Y. Zhao and C. Chen, *Nat. Nanotechnol.*, 2021, **16**, 708–716.
67 X. Lu, Y. Zhu, R. Bai, Z. Wu, W. Qian, L. Yang, R. Cai, H. Yan, T. Li, V. Pandey, Y. Liu, P. E. Lobie, C. Chen and T. Zhu, *Nat. Nanotechnol.*, 2019, **14**, 719–727.
68 Y. Shi, W. Gao, N. K. Lytle, P. Huang, X. Yuan, A. M. Dann, M. Ridinger-Saison, K. E. DelGiorno, C. E. Antal, G. Liang, A. R. Atkins, G. Erikson, H. Sun, J. Meisenhelder, E. Terenziani, G. Woo, L. Fang, T. P. Santisakultarm, U. Manor, R. Xu, C. R. Becerra, E. Borazanci, D. D. Von Hoff, P. M. Grandgenett, M. A. Hollingsworth, M. Leblanc, S. E. Umetsu, E. A. Collisson, M. Scadeng, A. M. Lowy, T. R. Donahue, T. Reya, M. Downes, R. M. Evans, G. M. Wahl, T. Pawson, R. Tian and T. Hunter, *Nature*, 2019, **569**, 131–135.
69 X. Yang, Y. Lin, Y. Shi, B. Li, W. Liu, W. Yin, Y. Dang, Y. Chu, J. Fan and R. He, *Cancer Res.*, 2016, **76**, 4124–4135.

70 Y. Kieffer, H. R. Hocine, G. Gentric, F. Pelon, C. Bernard, B. Bourachot, S. Lameiras, L. Albergante, C. Bonneau, A. Guyard, K. Tarte, A. Zinovyev, S. Baulande, G. Zalcman, A. Vincent-Salomon and F. Mechta-Grigoriou, *Cancer Discovery*, 2020, **10**, 1330–1351.
71 E. Sahai, I. Astsaturov, E. Cukierman, D. G. DeNardo, M. Egeblad, R. M. Evans, D. Fearon, F. R. Greten, S. R. Hingorani, T. Hunter, R. O. Hynes, R. K. Jain, T. Janowitz, C. Jorgensen, A. C. Kimmelman, M. G. Kolonin, R. G. Maki, R. S. Powers, E. Pure, D. C. Ramirez, R. Scherz-Shouval, M. H. Sherman, S. Stewart, T. D. Tlsty, D. A. Tuveson, F. M. Watt, V. Weaver, A. T. Weeraratna and Z. Werb, *Nat. Rev. Cancer*, 2020, **20**, 174–186.
72 M. H. Sherman, R. T. Yu, D. D. Engle, N. Ding, A. R. Atkins, H. Tiriac, E. A. Collisson, F. Connor, T. Van Dyke, S. Kozlov, P. Martin, T. W. Tseng, D. W. Dawson, T. R. Donahue, A. Masamune, T. Shimosegawa, M. V. Apte, J. S. Wilson, B. Ng, S. L. Lau, J. E. Gunton, G. M. Wahl, T. Hunter, J. A. Drebin, P. J. O'Dwyer, C. Liddle, D. A. Tuveson, M. Downes and R. M. Evans, *Cell*, 2014, **159**, 80–93.
73 H. Lin, Y. Yu, L. Zhu, N. Lai, L. Zhang, Y. Guo, X. Lin, D. Yang, N. Ren, Z. Zhu and Q. Dong, *Redox Biol.*, 2023, **59**, 102601.
74 C. Szabo, C. Coletta, C. Chao, K. Modis, B. Szczesny, A. Papapetropoulos and M. R. Hellmich, *Proc. Natl. Acad. Sci. U. S. A.*, 2013, **110**, 12474–12479.
75 B. Su, R. Wang, Z. Xie, H. Ruan, J. Li, C. Xie, W. Lu, J. Wang, D. Wang and M. Liu, *Small*, 2018, **14**, 1702331.
76 Z. Shen, T. Liu, Y. Li, J. Lau, Z. Yang, W. Fan, Z. Zhou, C. Shi, C. Ke, V. I. Bregadze, S. K. Mandal, Y. Liu, Z. Li, T. Xue, G. Zhu, J. Munasinghe, G. Niu, A. Wu and X. Chen, *ACS Nano*, 2018, **12**, 11355–11365.
77 L. Wang, W. Jiang, L. Xiao, H. Li, Z. Chen, Y. Liu, J. Dou, S. Li, Q. Wang, W. Han, Y. Wang and H. Liu, *ACS Nano*, 2020, **14**, 8459–8472.
78 Y. Zhang, X. Du, S. Liu, H. Yan, J. Ji, Y. Xi, X. Yang and G. Zhai, *Biomaterials*, 2021, **278**, 121135.
79 L. Tang, T. M. Fan, L. B. Borst and J. Cheng, *ACS Nano*, 2012, **6**, 3954–3966.
80 L. Tang, X. Yang, Q. Yin, K. Cai, H. Wang, I. Chaudhury, C. Yao, Q. Zhou, M. Kwon, J. A. Hartman, I. T. Dobrucki, L. W. Dobrucki, L. B. Borst, S. Lezmi, W. G. Helferich, A. L. Ferguson, T. M. Fan and J. Cheng, *Proc. Natl. Acad. Sci. U. S. A.*, 2014, **111**, 15344–15349.
81 Z. Song, T. Liu, H. Lai, X. Meng, L. Yang, J. Su and T. Chen, *ACS Nano*, 2022, **16**, 4379–4396.
82 X. Wang, X. Wang, Q. Yue, H. Xu, X. Zhong, L. Sun, G. Li, Y. Gong, N. Yang, Z. Wang, Z. Liu and L. Cheng, *Nano Today*, 2021, **39**, 101170.
83 S. Luan, R. Xie, Y. Yang, X. Xiao, J. Zhou, X. Li, P. Fang, X. Zeng, X. Yu, M. Chen, H. Gao and Y. Yuan, *Small*, 2022, **18**, 2200115.
84 C. Perez-Campana, V. Gomez-Vallejo, M. Puigivila, A. Martin, T. Calvo-Fernandez, S. E. Moya, R. F. Ziolo, T. Reese and J. Llop, *ACS Nano*, 2013, **7**, 3498–3505.
85 R. K. Kankala, C. G. Liu, D. Y. Yang, S. B. Wang and A. Z. Chen, *Chem. Eng. J.*, 2020, **383**, 123138.
86 E. Blanco, H. Shen and M. Ferrari, *Nat. Biotechnol.*, 2015, **33**, 941–951.
87 S. Zhang, C. Sun, J. Zeng, Q. Sun, G. Wang, Y. Wang, Y. Wu, S. Dou, M. Gao and Z. Li, *Adv. Mater.*, 2016, **28**, 8927–8936.
88 Z. Li, Z. Chu, J. Yang, H. Qian, J. Xu, B. Chen, T. Tian, H. Chen, Y. Xu and F. Wang, *ACS Nano*, 2022, **16**, 15471–15483.
89 S. Hua, J. He, F. Zhang, J. Yu, W. Zhang, L. Gao, Y. Li and M. Zhou, *Biomaterials*, 2021, **268**, 120590.
90 T. Liu, L. Tong, N. Lv, X. Ge, Q. Fu, S. Gao, Q. Ma and J. Song, *Adv. Funct. Mater.*, 2019, **29**, 1806429.
91 H. Jin, T. Zhu, X. Huang, M. Sun, H. Li, X. Zhu, M. Liu, Y. Xie, W. Huang and D. Yan, *Biomaterials*, 2019, **211**, 68–80.
92 P. Xiao, W. Xie, J. Zhang, Q. Wu, Z. Shen, C. Guo, Y. Wu, F. Wang, B. Z. Tang and D. Wang, *J. Am. Chem. Soc.*, 2023, **145**, 334–344.
93 Y. Wang, J. Nie, W. Fang, L. Yang, Q. Hu, Z. Wang, J. Z. Sun and B. Z. Tang, *Chem. Rev.*, 2020, **120**, 4534–4577.
94 J. Luo, Z. Xie, J. W. Lam, L. Cheng, H. Chen, C. Qiu, H. S. Kwok, X. Zhan, Y. Liu, D. Zhu and B. Z. Tang, *Chem. Commun.*, 2001, 1740–1741.
95 L. Zhang, H. Su, H. Wang, Q. Li, X. Li, C. Zhou, J. Xu, Y. Chai, X. Liang, L. Xiong and C. Zhang, *Theranostics*, 2019, **9**, 1893–1908.
96 H. Petek, *ACS Nano*, 2014, **8**, 5–13.
97 V. P. Chauhan, Z. Popović, O. Chen, J. Cui, D. Fukumura, M. G. Bawendi and R. K. Jain, *Angew. Chem., Int. Ed.*, 2011, **50**, 11417–11420.
98 N. Wang, J. Li, J. Wang, D. Nie, X. Jiang, Y. Zhuo and M. Yu, *J. Controlled Release*, 2022, **350**, 886–897.
99 Z. Zhang, C. Liu, C. Li, W. Wu and X. Jiang, *Research*, 2019, 2391486.
100 H. Zhao, Y. Li, B. Zhao, C. Zheng, M. Niu, Q. Song, X. Liu, Q. Feng, Z. Zhang and L. Wang, *Acta Pharm. Sin. B*, 2023, **13**, 3892–3905.
101 Z. Dai, Q. Wang, J. Tang, R. Qu, M. Wu, H. Li, Y. Yang, X. Zhen and C. Yu, *Biomaterials*, 2022, **284**, 121533.
102 Y. Hua, Z. H. Shao, A. Zhai, L. J. Zhang, Z. Y. Wang, G. Zhao, F. Xie, J. Q. Liu, X. Zhao, X. Chen and S. Q. Zang, *ACS Nano*, 2023, **17**, 7837–7846.
103 P. Xie and P. Liu, *Carbohydr. Polym.*, 2022, **275**, 118760.
104 Y. Chen, M. Gao, L. Zhang, E. Ha, X. Hu, R. Zou, L. Yan and J. Hu, *Adv. Healthcare Mater.*, 2021, **10**, 2001665.
105 H. Duan, H. Guo, R. Zhang, F. Wang, Z. Liu, M. Ge, L. Yu, H. Lin and Y. Chen, *Biomaterials*, 2020, **256**, 120206.
106 Y. Yang, T. Hu, Y. Bian, F. Meng, S. Yu, H. Li, Q. Zhang, L. Gu, X. Weng, C. Tan and R. Liang, *Adv. Mater.*, 2023, **35**, 2211205.
107 H. Zhang, L. Zhang, Z. Cao, S. Cheong, C. Boyer, Z. Wang, S. L. J. Yun, R. Amal and Z. Gu, *Small*, 2022, **18**, 2200299.
108 Z. Zhou, Y. Liu, M. Zhang, C. Li, R. Yang, J. Li, C. Qian and M. Sun, *Adv. Funct. Mater.*, 2019, **29**, 1904144.

109 J. Li, X. Li, Y. Zhang, K. Jin, Y. Yuan, R. Ming, Y. Yang and T. Chen, *Nano Res.*, 2023, **16**, 873–881.
110 W. Dang, B. Ma, B. Li, Z. Huan, N. Ma, H. Zhu, J. Chang, Y. Xiao and C. Wu, *Biofabrication*, 2020, **12**, 025005.
111 Q. W. Chen, J. W. Wang, X. N. Wang, J. X. Fan, X. H. Liu, B. Li, Z. Y. Han, S. X. Cheng and X. Z. Zhang, *Angew. Chem., Int. Ed.*, 2020, **59**, 21562–21570.
112 K. Wang, M. Jiang, J. Zhou, Y. Liu, Q. Zong and Y. Yuan, *ACS Nano*, 2022, **16**, 721–735.
113 B. Wu, J. Fu, Y. Zhou, S. Luo, Y. Zhao, G. Quan, X. Pan and C. Wu, *Acta Pharm. Sin. B*, 2020, **10**, 2198–2211.
114 X. Jiang, M. Lee, J. Xia, T. Luo, J. Liu, M. Rodriguez and W. Lin, *ACS Nano*, 2022, **16**, 21417–21430.
115 C. Xu, Y. Yan, J. Tan, D. Yang, X. Jia, L. Wang, Y. Xu, S. Cao and S. Sun, *Adv. Funct. Mater.*, 2019, **29**, 1808146.
116 C. Wang, X. Wang, W. Zhang, D. Ma, F. Li, R. Jia, M. Shi, Y. Wang, G. Ma and W. Wei, *Adv. Mater.*, 2022, **34**, 2107150.
117 Z. Chu, T. Tian, Z. Tao, J. Yang, B. Chen, H. Chen, W. Wang, P. Yin, X. Xia, H. Wang and H. Qian, *Bioact. Mater.*, 2022, **17**, 71–80.
118 Y. Chang, Y. Cheng, R. Zheng, X. Wu, P. Song, Y. Wang, J. Yan and H. Zhang, *Nano Today*, 2021, **38**, 101110.
119 Z. Wang, Y. Wang, X. Sun, J. Zhou, X. Chen, J. Xi, L. Fan, J. Han and R. Guo, *Small*, 2022, **18**, 2200588.
120 Q. Lu, T. Lu, M. Xu, L. Yang, Y. Song and N. Li, *Biomaterials*, 2020, **257**, 120236.
121 Y. Wang, Z. Li, Y. Hu, J. Liu, M. Guo, H. Wei, S. Zheng, T. Jiang, X. Sun, Z. Ma, Y. Sun, F. Besenbacher, C. Chen and M. Yu, *Biomaterials*, 2020, **255**, 120167.
122 Z. Sun, T. Wang, J. Wang, J. Xu, T. Shen, T. Zhang, B. Zhang, S. Gao, C. Zhao, M. Yang, F. Sheng, J. Yu and Y. Hou, *J. Am. Chem. Soc.*, 2023, **145**, 11019–11032.
123 Z. Chu, H. Chen, P. Wang, W. Wang, J. Yang, J. Sun, B. Chen, T. Tian, Z. Zha, H. Wang and H. Qian, *ACS Nano*, 2022, **16**, 4917–4929.
124 W. Wu, Y. Pu, S. Gao, Y. Shen, M. Zhou, H. Yao and J. Shi, *Nano-Micro Lett.*, 2022, **14**, 220.
125 Y. Zhang, J. Zhao, L. Zhang, Y. Zhao, Y. Zhang, L. Cheng, D. Wang, C. Liu, M. Zhang, K. Fan and M. Zhang, *Nano Today*, 2023, **49**, 101798.
126 M. Ma, Y. Chen, M. Zhao, J. Sui, Z. Guo, Y. Yang, Z. Xu, Y. Sun, Y. Fan and X. Zhang, *Biomaterials*, 2021, **271**, 120741.
127 X. Li, H. Li, C. Zhang, A. Pich, L. Xing and X. Shi, *Bioact. Mater.*, 2021, **6**, 3473–3484.
128 X. Liu, W. Zhan, G. Gao, Q. Jiang, X. Zhang, H. Zhang, X. Sun, W. Han, F.-G. Wu and G. Liang, *J. Am. Chem. Soc.*, 2023, **145**, 7918–7930.
129 Y. Yang, B. Wang, X. Zhang, H. Li, S. Yue, Y. Zhang, Y. Yang, M. Liu, C. Ye, P. Huang and X. Zhou, *Adv. Mater.*, 2023, **35**, 2211337.
130 B. Chen, C. Zhang, W. Wang, Z. Chu, Z. Zha, X. He, W. Zhou, T. Liu, H. Wang and H. Qian, *ACS Nano*, 2020, **14**, 14919–14928.
131 Y. Tang, H. K. Bisoyi, X. M. Chen, Z. Liu, X. Chen, S. Zhang and Q. Li, *Adv. Mater.*, 2023, **35**, 2300232.
132 C. Zhang, D. Li, P. Pei, W. Wang, B. Chen, Z. Chu, Z. Zha, X. Yang, J. Wang and H. Qian, *Biomaterials*, 2020, **237**, 119835.
133 J. Ruan, H. Liu, B. Chen, F. Wang, W. Wang, Z. Zha, H. Qian, Z. Miao, J. Sun, T. Tian, Y. He and H. Wang, *ACS Nano*, 2021, **15**, 11428–11440.
134 Y. Zhang, Y. Sun, X. Dong, Q.-S. Wang, D. Zhu, L. Mei, H. Yan and F. Lv, *ACS Nano*, 2022, **16**, 6359–6371.
135 R. Zhang, P. Zang, D. Yang, J. Li, N. Hu, S. Qu and P. Yang, *Adv. Funct. Mater.*, 2023, **33**, 2300522.
136 S. Huo, P. Zhao, Z. Shi, M. Zou, X. Yang, E. Warszawik, M. Loznik, R. Goestl and A. Herrmann, *Nat. Chem.*, 2021, **13**, 131–139.
137 X. Liu, B. Yan, Y. Li, X. Ma, W. Jiao, K. Shi, T. Zhang, S. Chen, Y. He, X. J. Liang and H. Fan, *ACS Nano*, 2020, **14**, 1936–1950.
138 A. R. Smothers, J. R. Henderson, J. J. O'Connell, J. M. Stenbeck, D. Dean, T. G. Harvey and B. W. Booth, *Discover Oncol.*, 2023, **14**, 34.
139 S. Yao, X. Zhao, X. Wang, T. Huang, Y. Ding, J. Zhang, Z. Zhang, Z. L. Wang and L. Li, *Adv. Mater.*, 2022, **34**, 2109568.
140 T. Chen, T. Gu, L. Cheng, X. Li, G. Han and Z. Liu, *Biomaterials*, 2020, **255**, 120202.
141 G. He, Y. Li, M. R. Younis, L. H. Fu, T. He, S. Lei, J. Lin and P. Huang, *Nat. Commun.*, 2022, **13**, 6238.
142 P. Decuzzi and M. Ferrari, *Biophys. J.*, 2008, **94**, 3790–3797.
143 Y. Zhao, Y. Wang, F. Ran, Y. Cui, C. Liu, Q. Zhao, Y. Gao, D. Wang and S. Wang, *Sci. Rep.*, 2017, **7**, 4131.
144 S. Barua, J. W. Yoo, P. Kolhar, A. Wakankar, Y. R. Gokarn and S. Mitragotri, *Proc. Natl. Acad. Sci. U. S. A.*, 2013, **110**, 3270–3275.
145 P. Kolhar, A. C. Anselmo, V. Gupta, K. Pant, B. Prabhakarpandian, E. Ruoslahti and S. Mitragotri, *Proc. Natl. Acad. Sci. U. S. A.*, 2013, **110**, 10753–10758.
146 B. Godin, C. Chiappini, S. Srinivasan, J. F. Alexander, K. Yokoi, M. Ferrari, P. Decuzzi and X. Liu, *Adv. Funct. Mater.*, 2012, **22**, 4225–4235.
147 H. Liang, J. Guo, Y. Shi, G. Zhao, S. Sun and X. Sun, *Biomaterials*, 2021, **268**, 120530.
148 X. Huang, J. Pan, F. Xu, B. Shao, Y. Wang, X. Guo and S. Zhou, *Adv. Sci.*, 2021, **8**, 2003572.
149 X. Wei, M. Du, Z. Chen and Z. Yuan, *Cancers*, 2022, **14**, 4945.
150 C. R. Gurbatri, N. Arpaia and T. Danino, *Science*, 2022, **378**, 858–863.
151 M. Dougan and S. K. Dougan, *Nat. Med.*, 2019, **25**, 1030–1031.
152 J. X. Fan, M. T. Niu, Y. T. Qin, Y. X. Sun and X. Z. Zhang, *Adv. Drug Delivery Rev.*, 2022, **185**, 114296.
153 W. Jiang, Z. Zhang, Q. Wang, J. Dou, Y. Zhao, Y. Ma, H. Liu, H. Xu and Y. Wang, *Nano Lett.*, 2019, **19**, 4060–4067.
154 Y. Zhang, Q. Chen, Y. Zhu, M. Pei, K. Wang, X. Qu, Y. Zhang, J. Gao and H. Qin, *MedComm*, 2022, **3**, e192.

155 W. Lei, C. Yang, Y. Wu, G. Ru, X. He, X. Tong and S. Wang, *J. Nanobiotechnol.*, 2022, **20**, 45.
156 D. Zheng, J. Zhou, L. Qian, X. Liu, C. Chang, S. Tang, H. Zhang and S. Zhou, *Bioact. Mater.*, 2023, **22**, 567–587.
157 H. S. El-Sawy, A. M. Al-Abd, T. A. Ahmed, K. M. El-Say and V. P. Torchilin, *ACS Nano*, 2018, **12**, 10636–10664.
158 P. Xu, E. A. Van Kirk, Y. Zhan, W. J. Murdoch, M. Radosz and Y. Shen, *Angew. Chem., Int. Ed.*, 2007, **46**, 4999–5002.
159 Q. Hu, W. Sun, Y. Lu, H. N. Bomba, Y. Ye, T. Jiang, A. J. Isaacson and Z. Gu, *Nano Lett.*, 2016, **16**, 1118–1126.
160 X. Guan, Z. Guo, L. Lin, J. Chen, H. Tian and X. Chen, *Nano Lett.*, 2016, **16**, 6823–6831.
161 Q. Zhou, S. Shao, J. Wang, C. Xu, J. Xiang, Y. Piao, Z. Zhou, Q. Yu, J. Tang, X. Liu, Z. Gan, R. Mo, Z. Gu and Y. Shen, *Nat. Nanotechnol.*, 2019, **14**, 799–809.
162 X. Xie, Y. Feng, H. Zhang, Q. Su, T. Song, G. Yang, N. Li, X. Wei, T. Li, X. Qin, S. Li, C. Wu, X. Zhang, G. Wang, Y. Liu and H. Yang, *Bioact. Mater.*, 2022, **16**, 107–119.
163 K. Xiao, Y. Li, J. Luo, J. S. Lee, W. Xiao, A. M. Gonik, R. G. Agarwal and K. S. Lam, *Biomaterials*, 2011, **32**, 3435–3446.
164 Y. Yan, L. Zhou, Z. Sun, D. Song and Y. Cheng, *Bioact. Mater.*, 2022, **7**, 333–340.
165 J. Liu, J. Shi, W. Nie, S. Wang, G. Liu and K. Cai, *Adv. Healthcare Mater.*, 2020, **10**, 2001207.
166 S. Yang, C. Chen, Y. Qiu, C. Xu and J. Yao, *Biomaterials*, 2021, **268**, 120562.
167 S. He, X. Jia, S. Feng and J. Hu, *Small*, 2023, **19**, 2300078.
168 B. Ji, M. Wei and B. Yang, *Theranostics*, 2022, **12**, 434–458.
169 L. Huang, S. Zhao, J. Wu, L. Yu, N. Singh, K. Yang, M. Lan, P. Wang and J. S. Kim, *Coord. Chem. Rev.*, 2021, **438**, 213888.
170 W. N. Wang, C. X. Huang, C. Y. Zhang, M. L. Zhao, J. Zhang, H. J. Chen, Z. B. Zha, T. Zhao and H. S. Qian, *Appl. Catal., B*, 2018, **224**, 854–862.
171 X. Huang, Y. Lu, M. Guo, S. Du and N. Han, *Theranostics*, 2021, **11**, 7546–7569.
172 J. Lin, B. Xing and D. Jin, *Adv. Opt. Mater.*, 2023, **11**, 2300802.
173 G. Petroni, L. C. Cantley, L. Santambrogio, S. C. Formenti and L. Galluzzi, *Nat. Rev. Clin. Oncol.*, 2022, **19**, 114–131.
174 K. Wang and J. E. Tepper, *Ca-Cancer J. Clin.*, 2021, **71**, 437–454.
175 L. Xiao, B. Chen, W. Wang, T. Tian, H. Qian, X. Li and Y. Yu, *Adv. Sci.*, 2023, **10**, 2302141.
176 R. A. Chandra, F. K. Keane, F. E. M. Voncken and C. R. Thomas, *Lancet*, 2021, **398**, 171–184.
177 L. Galluzzi, M. J. Aryankalayil, C. N. Coleman and S. C. Formenti, *Nat. Rev. Clin. Oncol.*, 2023, **20**, 543–557.
178 Y. Wu, Y. Song, R. Wang and T. Wang, *Mol. Cancer*, 2023, **22**, 96.
179 B. Chen, L. Xiao, W. Wang, L. Xu, Y. Jiang, G. Zhang, L. Liu, X. Li, Y. Yu and H. Qian, *ACS Appl. Mater. Interfaces*, 2023, **15**, 33903–33915.
180 S. Son, J. H. Kim, X. Wang, C. Zhang, S. A. Yoon, J. Shin, A. Sharma, M. H. Lee, L. Cheng, J. Wu and J. S. Kim, *Chem. Soc. Rev.*, 2020, **49**, 3244–3261.
181 H. Gavilan, S. K. Avugadda, T. Fernandez-Cabada, N. Soni, M. Cassani, B. T. Mai, R. Chantrell and T. Pellegrino, *Chem. Soc. Rev.*, 2021, **50**, 11614–11667.
182 Y. Chao, G. Chen, C. Liang, J. Xu, Z. Dong, X. Han, C. Wang and Z. Liu, *Nano Lett.*, 2019, **19**, 4287–4296.
183 W. Wang, F. Li, S. Li, Y. Hu, M. Xu, Y. Zhang, M. I. Khan, S. Wang, M. Wu, W. Ding and B. Qiu, *J. Mater. Sci. Technol.*, 2021, **81**, 77–87.
184 J. C. Moser, E. Salvador, K. Deniz, K. Swanson, J. Tuszynski, K. W. Carlson, N. K. Karanam, C. B. Patel, M. Story, E. Lou and C. Hagemann, *Cancer Res.*, 2022, **82**, 3650–3658.
185 Z. S. Miripour, A. Ghahremani, K. Karimi, F. Jahanbakhsh, F. Abbasvandi, P. Hoseinpour, M. Parniani and M. Abdolahad, *Med. Oncol.*, 2023, **40**, 117.
186 S. Khan, A. Hasan, F. Attar, M. M. N. Babadaei, H. A. Zeinabad, M. Salehi, M. Alizadeh, M. Hassan, H. Derakhshankhah, M. R. Hamblin, Q. Bai, M. Sharifi, M. Falahati and T. L. M. ten Hagen, *J. Controlled Release*, 2021, **338**, 341–357.
187 Y. Jiang, C. Feng, W. Wang, H. Qian and L. Xu, *Adv. Mater. Technol.*, 2023, **8**, 2300688.
188 J. Yang, Z. Chu, Y. Jiang, W. Zheng, J. Sun, L. Xu, Y. Ma, W. Wang, M. Shao and H. Qian, *Adv. Healthcare Mater.*, 2023, **12**, 2300725.
189 Z. Sartawi, C. Blackshields and W. Faisal, *J. Controlled Release*, 2022, **348**, 186–205.
190 H. Teymourian, F. Tehrani, K. Mahato and J. Wang, *Adv. Healthcare Mater.*, 2021, **10**, 2002255.
191 J. Yang, X. Liu, Y. Fu and Y. Song, *Acta Pharm. Sin. B*, 2019, **9**, 469–483.
192 F. Conforti, L. Pala, V. Bagnardi, G. Viale, T. De Pas, E. Pagan, R. D. Gelber and A. Goldhirsch, *Ann. Oncol.*, 2019, **30**, 653–655.
193 M. Fane and A. T. Weeraratna, *Nat. Rev. Cancer*, 2020, **20**, 89–106.
194 Y. Hoogstrate, K. Draaisma, S. A. Ghisai, L. van Hijfte, N. Barin, I. de Heer, W. Coppieters, T. P. P. van den Bosch, A. Bolleboom, Z. Gao, A. J. P. E. Vincent, L. Karim, M. Deckers, M. J. B. Taphoorn, M. Kerkhof, A. Weyerbrock, M. Sanson, A. Hoeben, S. Lukacova, G. Lombardi, S. Leenstra, M. Hanse, R. E. M. Fleischeuer, C. Watts, N. Angelopoulos, T. Gorlia, V. Golfinopoulos, V. Bours, M. J. van den Bent, P. A. Robe and P. J. French, *Cancer Cell*, 2023, **41**, 678–692.
195 W. Zou and D. R. Green, *Cell Metab.*, 2023, **35**, 1101–1113.
196 X. Zhang, Q. Zhao, J. Yang, T. Wang, F. Chen and K. Zhang, *Coord. Chem. Rev.*, 2023, **484**, 215115.
197 Q. Sun, M. Barz, B. G. De Geest, M. Diken, W. E. Hennink, F. Kiessling, T. Lammers and Y. Shi, *Chem. Soc. Rev.*, 2019, **48**, 351–381.
198 Y. Liu, Y. Wang, S. Song and H. Zhang, *Adv. Mater.*, 2021, **33**, 2103936.
199 H. J. Vaughan, J. J. Green and S. Y. Tzeng, *Adv. Mater.*, 2020, **32**, 1901081.
200 G. H. Lee, H. Moon, H. Kim, G. H. Lee, W. Kwon, S. Yoo, D. Myung, S. H. Yun, Z. Bao and S. K. Hahn, *Nat. Rev. Mater.*, 2020, **5**, 149–165.

201 Y. Hu, J. Wei, Y. Shen, S. Chen and X. Chen, *Ultrason. Sonochem.*, 2023, **94**, 106346.
202 V. Gadekar, Y. Borade, S. Kannaujia, K. Rajpoot, N. Anup, V. Tambe, K. Kalia and R. K. Tekade, *J. Controlled Release*, 2021, **330**, 372–397.
203 T. I. Janjua, Y. Cao, C. Yu and A. Popat, *Nat. Rev. Mater.*, 2021, **6**, 1072–1074.
204 P. J. Gawne, M. Ferreira, M. Papaluca, J. Grimm and P. Decuzzi, *Nat. Rev. Mater.*, 2023, **8**, 783–798.
205 N. Ni, X. Zhang, Y. Ma, J. Yuan, D. Wang, G. Ma, J. Dong and X. Sun, *Coord. Chem. Rev.*, 2022, **458**, 214415.
206 R. Zhao, X. Liu, X. Yang, B. Jin, C. Shao, W. Kang and R. Tang, *Adv. Mater.*, 2018, **30**, 1801304.
207 S. Liang, J. Yao, D. Liu, L. Rao, X. Chen and Z. Wang, *Adv. Mater.*, 2023, **35**, 2211130.
208 M. Saeed, F. Chen, J. Ye, Y. Shi, T. Lammers, B. G. De Geest, Z. P. Xu and H. Yu, *Adv. Mater.*, 2021, **33**, 2008094.